OFFICE OF NAVAL RESEARCH

Contract N00014-84-K-0021

TECHNICAL REPORT NO. 2

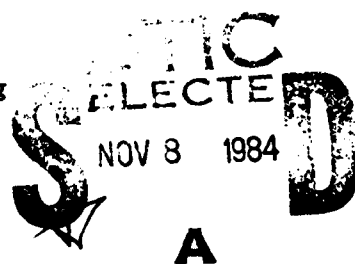RUBBER-MODIFIED EPOXIES: I. CURE, TRANSITIONS, AND MORPHOLOGY

by

L. C. Chan, J. K. Gillham, A. J. Kinloch and S. J. Shaw

for publication in

Advances in Chemistry Series, Number 209
American Chemical Society
Washington, D.C.

PRINCETON UNIVERSITY
Polymer Materials Program
Department of Chemical Engineering
Princeton, New Jersey 08544

October 1984

Principal Investigator
John K. Gillham
(609) 452-4694

REPORT DOCUMENTATION PAGE		READ INSTRUCTIONS BEFORE COMPLETING FORM
1. REPORT NUMBER Technical Report #2	2. GOVT ACCESSION NO. AD-A147377 N/A	3. RECIPIENT'S CATALOG NUMBER N/A
4. TITLE (and Subtitle) Rubber-Modified Epoxies: I. Cure, Transitions, and Morphology		5. TYPE OF REPORT & PERIOD COVERED April 1984 - October 1984
		6. PERFORMING ORG. REPORT NUMBER
7. AUTHOR(s) L. C. Chan, J. K. Gillham, A. J. Kinloch and S. J. Shaw		8. CONTRACT OR GRANT NUMBER(s) N00014-84-K-0021
9. PERFORMING ORGANIZATION NAME AND ADDRESS Polymer Materials Program Department of Chemical Engineering Princeton University, Princeton, NJ 08544		10. PROGRAM ELEMENT, PROJECT, TASK AREA & WORK UNIT NUMBERS
11. CONTROLLING OFFICE NAME AND ADDRESS U. S. Army Research Office Post Office Box 12211 Research Triangle Park, NC 27709		12. REPORT DATE October 1984
		13. NUMBER OF PAGES 56
14. MONITORING AGENCY NAME & ADDRESS(if different from Controlling Office)		15. SECURITY CLASS. (of this report) Unclassified
		15a. DECLASSIFICATION/DOWNGRADING SCHEDULE

16. DISTRIBUTION STATEMENT (of this Report)

Approved for public release; distribution unlimited.

17. DISTRIBUTION STATEMENT (of the abstract entered in Block 20, if different from Report)

NA

18. SUPPLEMENTARY NOTES

The view, opinions, and/or findings contained in this report are those of the author(s) and should not be construed as an official Department of the Army position, policy, or decision, unless so designated by other documentation.

19. KEY WORDS (Continue on reverse side if necessary and identify by block number)

Cure	Kinetics
Epoxies	Morphology
Fracture	Rubber Modified
Gelation	Vitrification
Glass Transition	

20. ABSTRACT (Continue on reverse side if necessary and identify by block number)

A methodology for investigating cure and its relationship to the development of morphology and transitions for rubber-modified thermosetting systems has been developed. An aromatic tetrafunctional diamine-cured diglycidyl ether of bis-phenol A epoxy resin [maximum glass transition temperature $(_{E}T_{g\infty})$ = 167°C] was modified separately with two reactive liquid rubbers; i.e., a prereacted carboxyl-terminated rubber and an amino-terminated rubber. In order to develop fully cured but distinct cure-dependent morphologies, the systems were cured isothermally at different temperatures until reactions ceased and then were postcured by heating

DD FORM 1473 EDITION OF 1 NOV 65 IS OBSOLETE

above $_ET_{g\infty}$. The maximum glass transition temperature of the matrix and the volume fraction of dispersed phase for the amino-terminated rubber-modified system were particularly sensitive to cure conditions in consequence of complications in the cure chemistry.

RUBBER-MODIFIED EPOXIES:

I. CURE, TRANSITIONS, AND MORPHOLOGY

L. C. Chan and J. K. Gillham
Polymer Materials Program
Department of Chemical Engineering
Princeton University
Princeton, NJ 08544 USA

and

A. J. Kinloch and S. J. Shaw
Ministry of Defence
Royal Armament Research and Development
Establishment (Waltham Abbey)
Essex EN9 IBP U.K.

the maximum glass transition temperature

ABSTRACT

A methodology for investigating cure and its relationship to the development of morphology and transitions for rubber-modified thermosetting systems has been developed. An aromatic tetrafunctional diamine-cured diglycidyl ether of bisphenol A epoxy resin [maximum glass transition temperature $(_ET_{g\infty})$ = 167°C] was modified separately with two reactive liquid rubbers; i.e., a prereacted carboxyl-terminated rubber and an amino-terminated rubber. In order to develop fully cured but distinct cure-dependent morphologies, the systems were cured isothermally at different temperatures until reactions ceased and then were postcured by heating above $T_{g\infty}$. The maximum glass transition temperature of the matrix and the volume fraction of dispersed phase for the amino-terminated rubber-modified system were particularly sensitive to cure conditions in consequence of complications in the cure chemistry.

INTRODUCTION

In common with other high T_g thermosets, unmodified cured epoxy resins are brittle materials. The crack resistance can be improved by the addition of reactive liquid rubber to uncured neat epoxy systems (1-3). In-situ phase separation occurs during cure; the cured rubber-modified epoxy resins consist of finely dispersed rubber-rich domains (~ 0.1 - 5 μm) bonded to the epoxy matrix. Improvement of fracture energy is dependent on the particle size, volume fraction, and size distribution of the dispersed phase, and on the chemical structures of the matrix and the dispersed phase (4-14). Shear deformation (2,7), void formation (6,7), crazing (2-4), and rubber tear (9,10) have been proposed as toughening mechanisms.

Cure of an initially homogeneous solution of epoxy resin/curing agent/rubber generally involves the sequential processes of phase separation, gelation, and vitrification. During cure, phase separation of the rubber occurs due to the increase of molecular weight which lowers the compatibility of the rubber with the epoxy system, and is eventually quenched by the high viscosity accompanying gelation or vitrification (5). The development of morphology is dependent on the rates of nucleation and growth of the dispersed phase, compatibility of the rubber, and the rate of cure reactions (5,15). Since these factors are temperature-dependent, cure conditions may have a profound effect on the morphology and consequently on the mechanical behavior of the cured resin. Despite the potential implications, the effect of cure conditions on the properties of rubber-modified epoxies has scarcely been studied. If a range of morphologies can be obtained from a single rubber-

modified epoxy formulation through control of cure conditions, relationships between mechanical properties and morphology may be better understood.

The main objective of this report is to discuss the cure process and its relationship to the development of morphology and transitions for two rubber-modified epoxy systems using an unmodified neat system as the control sample. The effect of cure conditions on the mechanical properties for the cured specimens is discussed in a complementary paper (16). In an attempt to develop and arrest fully cured but distinct cure-dependent morphologies, the systems were cured isothermally at different temperatures (T_{cure}) to well beyond gelation and vitrification and then were postcured by heating above the maximum glass transition temperature ($_ET_{g\infty}$) of the system to complete the reactions of the matrix. An aromatic tetrafunctional diamine-cured diglycidyl ether of bisphenol A (DGEBA)-type epoxy resin was selected as the neat system because of its high $_ET_{g\infty}$ (167°C). The two rubbers were a prereacted carboxyl-terminated rubber and an amino-terminated rubber, both being made from the same copolymer of butadiene and acrylonitrile containing 17% acrylonitrile. The chemistry of cure would be expected to be the same for the neat and prereacted carboxyl-terminated rubber-modified systems, whereas competing cure reactions should be introduced in using the amino-terminated rubber. A preliminary report has been published (17).

A methodology for understanding and comparing cure behavior and properties of the cured state for rubber-modified thermosets has been developed in this work. The first part involves monitoring cure by torsional braid analysis (TBA) to give gelation and vitrification times at different

cure temperatures, assessing the kinetics of phase separation by complementary turbidity measurements, and summarizing the data in a time-temperature-transformation (TTT) isothermal cure diagram. The second part summarizes transition temperatures after extended isothermal cure, and also after post-cure, in plots of transition temperatures versus the isothermal cure temperature. The third part involves assessing the relative amounts of dissolved and phase-separated rubber from the depression of the glass transition temperature of the fully cured system ($_ET_{g\infty}$). The amount of the phase-separated rubber is then compared with that obtained from morphological examination using transmission electron microscopy (TEM). In the current work, an apparent inconsistency in the amount of dissolved versus phase-separated rubber for the amino-terminated rubber-modified system led to considerations of the influence of time-temperature cure paths on the chemistry of cure of the system.

EXPERIMENTAL

Materials

The chemical structures of the materials are shown in Figure 1. The base resin and curing agent for the two rubber-modified epoxy systems were: a diglycidyl ether of bisphenol A (DGEBA) resin (DER 331, Dow Chemical Co., epoxy equivalent weight = 190 gm) and trimethylene glycol di-p-aminobenzoate ("TMAB", i.e., Polacure 740M, Polaroid Corp., NH equivalent weight = 78.5 gm), respectively. DER 331/TMAB was selected because of the high T_g of the fully cured neat system ($_ET_{g\infty}$ = 167°C) and the nonvolatility (m.p. = 125°C; b.p. > 250°C), solubility, and health characteristics of TMAB.

The first system, denoted DTK-293, was modified with a commercial prereacted carboxyl-terminated butadiene-acrylonitrile copolymer containing 17% acrylonitrile (AN) content ("K-293", Spencer Kellog Co., epoxy equivalent weight = 340 gm). The K-293 rubber had been made by reacting a carboxyl-terminated rubber (CTBNx8, B. F. Goodrich Chemical Co., AN content = 17%, COOH equivalent weight = 1850 gm) with excess of DGEBA resin. One mole of K-293 contains approximately 0.44 mole of CTBNx8 rubber and 0.56 mole of DGEBA resin. The second system, denoted DTAx16, was modified with a commercial amino-terminated butadiene-acrylonitrile copolymer containing 17% AN (ATBNx16, B. F. Goodrich Chemical Co., NH equivalent weight = 850 gm). The ATBNx16 rubber had been made by reacting the CTBNx8 rubber with N-(2-aminoethyl)piperazine (AEP) (13). The ATBN rubber used in the present work contained a residual amount of AEP (3% by weight) from its synthesis. Since both rubbers, K-293 and ATBNx16, were made from the same CTBN rubber, the molecular weights and the T_g's of the rubbers are approximately the same $(T_g \cong -50°C)$. The formulations for the neat system and the two rubber-modified epoxy systems containing 15 phr of rubber are tabulated in Table I.

Specimen Preparation

A mixture of liquid epoxy resin and liquid rubber (for modified systems) was heated to 120°C in an open beaker and the solid curing agent was added and dissolved with the aid of mechanical stirring for 5 minutes. The solution was degassed at 100°C for 25 minutes in a preheated vacuum oven at a pressure of about 1 torr. A small part of this degassed mixture was dissolved in methyl

ethyl ketone in a volume ratio of 1 to 4 for the TBA experiments. The main batch of the degassed mixture was then poured into a preheated (at T_{cure}) mold [pre-coated with a release agent (QZ 13, Ciba-Geigy Chemical Co.) (18)], and cured in an air oven to prepare a casting (220 x 220 x 6 mm) for morphological and mechanical studies (16). The open end of the mold was sealed with a plug made of silicone rubber (RTV, General Electric Co.) in an attempt to minimize exposure to air during cure.

After prolonged isothermal cure, TBA specimens were postcured by heating to and from 240°C at a rate of 1.5°C/minute (see later). In contrast, the casting was postcured by heating the mold from the cure temperature to 1⁻ at 1.5°C/minute and holding at 170°C for 5 hours. Values of the maximum transition temperature ($_ET_{g\infty}$) obtained from strip specimens (16), which had been machined from the casting, were the same as those obtained from the TBA experiments. This indicates that the casting had been fully cured by the postcure step. The morphology of the cured specimens was not expected to be altered by the postcure process because the cure reactions had proceeded to well beyond gelation, and a slow heating rate had been used in postcuring.

Torsional Braid Analysis (TBA)

The transformation of a liquid epoxy formulation to solid thermoset polymer during the process of cure was monitored using a composite specimen in an automated torsional pendulum instrument [Torsional Braid Analysis (TBA), Plastics Analysis Instruments, Inc.] (19,20). The specimen was an inert

multifilamented glass braid impregnated with the reactive liquid. The pendulum was intermittently set into motion to generate a series of freely damped waves with a natural frequency of 0.05-5 Hz. The change of material behavior of the specimen was monitored as a function of time and/or temperature by measuring two dynamic mechanical properties, relative rigidity and logarithmic decrement, obtained from the frequency and decay constants that characterize each wave. The relative rigidity $[(1/P^2)$, where P is the period in seconds)] is directly proportional to the in-phase portion of the shear modulus (G'); the logarithmic decrement $[\Delta = \ln (A_i/A_{i+1})$, where A_i is the amplitude of the ith oscillation of a freely damped wave] is directly proportional to the rati' of the out-of-phase portion of the shear modulus (G") to G' ($\Delta \cong \pi G''/G' = \pi\tan\phi$, where ϕ is the phase angle between the stress and strain). At a selected temperature (T_{cure}), the specimen was cured until reactions were essentially quenched as indicated by the leveling off of the rigidity curve (although changes were still occurring in the mechanical damping). Transformations associated with changes of one state to another during cure were identified by the time of maxima (and the associated frequencies) in the logarithmic decrement plot. After prolonged isothermal cure, the dynamic mechanical spectrum of a cured specimen was obtained on cooling from T_{cure} to -170°C and heating to 240°C at a rate of 1.5°C/minute. A subsequent scan from 240 to -170°C was considered to provide the spectrum of the fully cured specimen. Transition temperatures were identified by the temperature of maxima (and the associated frequencies) in the logarithmic decrement plot during a temperature scan. All the TBA experiments in the present work were performed in helium.

Turbidity Study

In-situ phase separation was monitored from changes in light transmission through a sample consisting of a degassed epoxy formulation in a capillary glass tube (I.D. 1 mm) sandwiched between two heated copper blocks. The light beam was a He-Ne laser (λ = 632.8 nm, 0.95 mW; beam diameter $\sim$ 1 mm). The signal-to-noise ratio was amplified using a lock-in detection device (21) which consists of a chopper (Princeton Applied Research Co.: Model 191, chopping frequency = 200 Hz) and a lock-in amplifier (Princeton Applied Research Co.: Model 121). The chopper was placed between the laser and the sample. The intensity of light transmitted through the sample, which was monitored by a photodiode (Silicon Detector Co.: Model SD-444-11-11-171) connected to the lock-in amplifier, was recorded on an X-Y strip chart recorder. The light transmission set-up was covered by black cloth to minimize stray light from the background.

The initial mixtures of the two rubber-modified systems were optically clear within the cure temperature range (from 100 to 200°C), indicating that each of the two rubbers was compatible with the neat epoxy system at the beginning of cure. During cure, increase of molecular weight of the system lowered the compatibility of the rubber, and the mixture turned from optically clear to cloudy. The cloud point, which was defined as the first indication of decrease of light intensity transmitted through the sample, was taken to be the onset of phase separation. The end of phase separation was indicated by the leveling off of the light transmission curve. The light transmitted through the sample was constant throughout cure for the neat system.

Morphological Study

Morphologies of cured specimens were examined by scanning electron microscopy (SEM) and transmission electron microscopy (TEM). The SEM micrographs were obtained from the fracture surfaces of cured specimens which had been coated with a thin layer (~ 600 Å) of gold using a high vacuum sputterer. The TEM micrographs were obtained from specimens which had been stained with osmium tetraoxide and microtomed at room temperature. The osmium tetraoxide reacted with the unsaturated double bonds of the rubber molecules and the rubbery domains appeared as black sections in the TEM micrographs. Two analytical methods were used to convert the distribution of the sections in the TEM micrographs to the corresponding distribution of particles, from which the volume fraction and mean diameter of the particles were calculated. The first method (Schwartz-Saltykov's) (22) is based on the distribution of section diameters in the TEM micrographs. The second method (Spektor's) (22) is based on the distribution of chord intercept lengths along random straight lines drawn in the TEM micrographs. In general, good overall agreement is to be expected from using the two methods; however, the details of the results may differ because of the inherent differences in the analyses (22). Twenty to thirty TEM micrographs were examined for each cure condition.

RESULTS AND DISCUSSION

1. Neat Epoxy System (DER 331/TMAB)

Transformations from liquid-to-rubber and rubber-to-glass were measured by gelation and vitrification times, respectively. Representative isothermal TBA cure spectra from low to high temperatures of cure (100 to 200°C) of DER 331/TMAB are shown in Figure 2.

At low cure temperatures three events are apparent in the logarithmic decrement as is demonstrated by the 100 and 120°C isothermal cure spectra. The first peak has been designated as gelation (liquid-to-rubber transformation), and generally corresponds to the onset of insolubility (which accompanies the incipient formation of the crosslinked network) as measured in gel fraction experiments (23). The shoulder before the gelation peak (which is less apparent at higher temperatures) has been attributed to an iso-viscous event which is due to the interaction of the liquid and the braid in the TBA experiment (19), and so will not be considered further in the present communication. The second peak in the logarithmic decrement, which is located in the middle of the rubber-to-glass transition region as indicated by the relative rigidity plot, has been designated as vitrification (rubber-to-glass transformation) (19). Physically, the vitrification peak in the TBA isother-mal cure spectrum corresponds to the state at which the glass transition tem-perature ($_ET_g$) of the epoxy resin has risen to T_{cure} (14,23). Beyond gelation and approaching vitrification, the increases in the crosslink density and average molecular weight cause a reduction of molecular mobility and chemical reactivity, and so the reactions of the epoxy system become diffusion controlled. Eventually, the reactions are quenched when the resin has become a glass: this is demonstrated by the continuous increase and the subsequent

leveling off of the relative rigidity plot (modulus) beyond the vitrification peak. The glass transition temperature has then risen to a temperature T_{cure} + δT. The difference (δT) between $_ET_g$ of the isothermally cured resin and T_{cure} arises from the distinction between the quenching of chemical reactions and the particular method of measurement of both $_ET_g$ and vitrification (24). It should be noted that δT is itself a function of T_{cure} (see later) and of time at T_{cure}. If T_{cure} is higher than the maximum glass transition temperature ($_ET_{g\infty}$) of the DER 331/TMAB epoxy system ($_ET_{g\infty}$ = 167°C) vitrification cannot occur and only the gelation peak is observed, as in the 170 and 200°C isothermal cure spectra; therefore, reactions of the epoxy resin will not be quenched. Completion of the reactions can only be attained at temperatures above ($_ET_{g\infty}$ - δT); in contrast, reactions will be quenched if T_{cure} is below ($_ET_{g\infty}$ - δT).

Gelation and vitrification times of the DER 331/TMAB epoxy system at different cure temperatures are presented in Figure 3 in the form of a time-temperature-transformation (TTT) isothermal cure diagram (19,23). It should be noted that the TTT diagrams presented in this work have not taken into account the changes which occurred during the preparation of the specimens (i.e. 120°C for 5 minutes and 100°C for 25 minutes). The TTT diagram shows that the gelation and vitrification curves cross at 75°C (the value of which was obtained from the intersection of the log time versus $1/T$ plots for gelation and vitrification). The temperature at which times to reach gelation and vitrification are the same has been denoted as $_{gel}T_g$ (19). If T_{cure} is below ($_{gel}T_g$ - δT) but above ($_ET_{go}$ - δT) [$_ET_{go}$ = T_g of the initial resin] the resin

will not gel on cure but will vitrify to form an ungelled thermoplastic glass of low molecular weight. $_ET_{go}$ for the DER 331/TMAB epoxy system is 2°C as determined from a TBA thermomechanical spectrum. If T_{cure} is between ($_{gel}T_g$ - δT) and $_ET_{g\infty}$, the resin will gel to form a gelled glass. However, if T_{cure} is above $_ET_{g\infty}$, the resin gels to form a gelled rubber but does not vitrify at the temperatures of cure (as discussed). The vitrification curve in TTT isothermal cure diagrams is generally S-shaped, with $_ET_{g\infty}$ and $_ET_{go}$ as the upper and lower boundaries, respectively (19). The time to vitrify reaches a minimum at a T_{cure} just below $_ET_{g\infty}$ because of the competing effects of increasing reaction rate constant and increasing extent of conversion for vitrification with increasing temperature. In contrast, the time to vitrify reaches a maximum at a T_{cure} just above $_ET_{go}$ because of the competing effects of decreasing viscosity and increasing reactivity with increasing temperature. In the present work for the DER 331/TMAB epoxy system, only the upper part of the S-shaped vitrification curve in the TTT isothermal cure diagram has been obtained experimentally because of the low reactivity of the neat system at low temperature. However, $_ET_{go}$ was measured directly in a temperature scan. In principle, the S-shaped vitrification curve and the gelation curve can be computed from the reaction kinetics, the conversions at gelation and vitrification, and the physical parameters of the system ($_ET_{go}$, $_ET_{g\infty}$ and $_{gel}T_g$) which are dependent on the chemical structure of the reactive constituents of the system (23).

Representative TBA thermomechanical spectra, obtained after prolonged isothermal cure (100 to 200°C), are shown in Figure 4. Thermomechanical spectra were obtained on cooling from T_{cure} to -170°C and heating to 240°C.

If T_{cure} is below ($_ET_{g\infty}$ - δT), the partially cured resin can be postcured at higher temperatures and a subsequent scan from 240 to -170°C is considered to provide the spectrum of the fully cured resin. Three relaxations are observed: the glass transition ($_ET_g$) at higher temperatures, a subzero secondary transition ($_ET_{sec}$) [which has been attributed to the motion of the -CH_2-$CH(OH)$-CH_2-O-group in the epoxy (25)], and a weak one below -100°C. The maximum values of $_ET_g$ and $_ET_{sec}$ obtained after heating to 240°C for the DER 331/TMAB system were 167°C ($_ET_{g\infty}$) and -39°C ($_ET_{sec\infty}$), respectively. Both $_ET_{g\infty}$ and $_ET_{sec\infty}$ are independent of T_{cure}, whereas $_ET_g$ and $_ET_{sec}$ increase with T_{cure} (Figure 5). For $T_{cure} \ll {_ET_{g\infty}}$, the values of $_ET_g$ after cure at T_{cure} are about 20°C higher than T_{cure}. The measured difference ($_ET_g$ - T_{cure}) varies with epoxy systems (26,27).

It is noteworthy that the relative rigidity plot for a fully cured specimen crosses over that for the partially cured specimen: this is demonstrated in Figure 4a for the 100 and 120°C cured specimens. This implies that the modulus at room temperature (which is below the crossover temperature) for a cured specimen is lower the higher the $_ET_g$ and extent of conversion (crosslinking density). For other high T_g epoxy systems, the decrease in room temperature (RT) modulus with increasing extent of cure is paralleled by corresponding decreases in RT density, and increases in RT equilibrium levels of absorbed water (19,28). A common basis for these interrelated phenomena (28) is the increasing free volume at RT with increasing extent of cure (29).

2. Prereacted Carboxyl-Terminated Rubber-Modified Epoxy System (DTK-293)

The rubber used in this system is a commercially available prereacted carboxyl-terminated rubber copolymer of butadiene and acrylonitrile. The cure chemistry of the DTK-293 and neat systems are expected to be similar since the reactive functional end groups are the same. Representative TBA isothermal cure spectra from low to high temperatures of cure (100 to 200°C) are presented in Figure 6. As for the neat system, the isothermal cure spectra of the DTK-293 system displayed gelation and vitrification peaks, the times of which are summarized in the form of a TTT isothermal cure diagram (Figure 7). The initial glass transition temperatures of the DTK-293 and the neat systems were the same (i.e. $_E T_{go}$ = 2°C). Since the lowest temperature of cure was 100°C, only the upper part of the TTT diagram is shown. For comparison, the corresponding part of the TTT diagram for the neat system is also included. In general, the TTT diagram for the DTK-293 system follows the same pattern as that for the neat system. The times to gelation and activation energy of gelation (ΔE), obtained by plotting the gelation times in an Arrhenius manner (not shown), are also similar for the two systems. The activation energy of gelation for the DTK-293 system was found to be 14.2 kcal/mole compared to 14.1 kcal/mole for the neat system. However, the values of $_E T_{g\infty}$ for the DTK-293 system are not constant and are represented by a shaded band in the TTT diagram, the width of which represents the range of $_E T_{g\infty}$ due to different cure conditions.

The light transmission results are included in the TTT isothermal cure diagram (Figure 8). The time for onset of phase separation (cloud point)

decreases with increase of T_{cure}. A line denoting 90% decrease of the initial
light intensity is also included to provide an estimate of how rapidly the
morphology develops: most of the phase separation of the dispersed phase
occurred well before gelation, although some changes were observed afterwards
as has been reported (20,31).

Representative thermomechanical spectra (Figure 9) show four relaxation
processes in the logarithmic decrement plots: a high temperature relaxa-
tion associated with T_g of the epoxy matrix ($_ET_g$); a broad relaxation at about
-40°C; a relaxation at about -50°C associated with the T_g of the rubbery phase
($_RT_g$); and one below $_RT_g$. It is difficult to correlate the volume fraction of
the rubbery phase with the intensity of the relaxation associated with $_RT_g$ as
in other reports (4,5,32) because of the overlapping of $_RT_g$ with other pro-
cesses. The $_RT_g$ loss peaks were found to be located at or below the T_g of
the unreacted liquid rubber even though the rubber in the dispersed phase was
chemically combined with the epoxy resin. The suppression of $_RT_g$ is presu-
mably a consequence of the triaxial stresses induced on the rubbery domains
resulting from differences of thermal expansion coefficients of the two
phases (5).

Values of $_ET_g$, and $_ET_{g\infty}$ versus T_{cure} for the DTK-293 and neat systems
are shown in Figure 10 and are included in Table II. Values of $_ET_{g\infty}$ for the
rubber-modified system were lower than that for the neat system by 4 to 6°C.
The decrease of $_ET_{g\infty}$ for cured rubber-modified epoxy systems is considered to
arise from incomplete phase separation; the dissolved rubber plasticizes the
epoxy matrix. In principle, the amount of rubber dissolved versus phase-

separated can be determined from the values of $_ET_{g\infty}$ of the rubber-modified and the neat systems, and the T_g of the rubber, if it is assumed that the chemical structures of the epoxy matrices for the two systems are similar. In the present work, the Fox equation (33) was used to estimate the amount of dissolved rubber:

$$\frac{1}{T_{gm}} = \frac{W_1}{T_{g1}} + \frac{W_2}{T_{g2}}$$

where
$T_{gm} = _ET_{g\infty}$ of the rubber-modified epoxy matrix

$T_{g1} = _ET_{g\infty}$ of the neat system

$T_{g2} = T_g$ of the unreacted rubber (200 K = -50°C)

W_1, W_2 = weight fractions of epoxy and rubber in the rubber-modified epoxy matrix, respectively.

The weight fraction of the phase-separated rubber was obtained from the mass balance of W_2 calculated from the above equation and the rubber used in the formulation (W_O = 9.68%). The weight fraction was converted to volume fraction of phase-separated rubber from the densities of the rubber (0.948 gm/c.c.) and the fully cured neat epoxy specimen (1.218 gm/c.c.). The volume fraction of the dispersed phase (V_f^*) was then obtained from the calculated phase-separated rubber by assuming each rubber molecule was capped with two epoxy monomers in the dispersed phase. The values of the volume fraction of the dispersed phase determined from the decrease of $_ET_{g\infty}$ (Table III) were similar to those determined from TEM micrographs (see later).

Values of $_ET_{g\infty}$ for the rubber-modified DTK-293 system appeared to be only slightly dependent on cure conditions (Figure 10) varying from 163°C when cured at 100°C to 161°C when cured at 200°C. The narrow range of $_ET_{g\infty}$ suggests that the extent of phase separation was insensitive to cure conditions. This is confirmed by the TEM micrographs of the 100 (Figure 11a) and 200°C (Figure 11b) cured specimens. The volume fractions of the dispersed phase (V_f) for the two specimens were approximately the same ($V_f \sim 0.11$ for 100°C and $V_f \sim 0.13$ for 200°C) according to both Schwartz-Saltykov's diameter (22) and Spektor's chord methods (22) (Table III), although the size distributions for the two specimens were different. Both methods revealed that the 100 and 200°C cured specimens displayed a unimodal distribution of particle size; and that the mean diameter (d) of the particles for the 100°C cured specimen was smaller than that for the 200°C cured specimen (Table III). The size distributions of the two specimens obtained by using Schwartz-Saltykov's diameter method are shown in Figure 12. The variation of domain sizes with cure conditions is caused presumably by the effect of temperature on the rates of nucleation and growth of the dispersed phase (5, 15). At low temperatures of cure, high nucleation rate and high viscosity (low growth rate) will probably give rise to a system with smaller but more numerous particles. On the other hand, low nucleation rate and low viscosity (high growth rate) at high temperatures of cure will give rise to a system with larger but less numerous particles.

The apparently higher value of mean diameter (d) of the particles for the 200°C cured specimen determined by Spektor's method (Table III) may be a

consequence of the underestimation of the percentage of smaller particles, since smaller sections are less likely to be intersected than larger sections by straight lines drawn across the TEM micrographs. The problem is more acute for the 200°C cured specimen because of its wide range of particle sizes (Figure 12).

3.   Amino-Terminated Rubber-Modified Epoxy System (DTAx16)

The rubber used in this system is a commercially available amino-terminated liquid rubber copolymer of butadiene and acrylonitrile. The ATBN rubber usually contains a residual amount of N-(2-aminoethyl)piperazine (AEP) since it is made by reacting a CTBN rubber with AEP (13). The AEP content for the sample of ATBN rubber used in the present work was estimated to be about 3% by weight. This value was obtained from information provided by the manufacturer on the NH equivalent weights of the residue-free ATBN molecule (~ 1900 gm/NH eq.), AEP (~ 43 gm/NH eq.), and the ATBN rubber with its residual AEP (~ 850 gm/NH eq.).

Representative isothermal TBA cure spectra from low to high temperatures (100 to 200°C) for the DTAx16 system are presented in Figure 13. The times to gelation and vitrification for the DTAx16 system and the neat system are summarized in Figure 14 in the form of a TTT isothermal cure diagram. $_E T_{go}$ of the DTAx16 system was 2°C, just as for the neat and DTK-293 systems. In contrast to the DTK-293 system, the times to gelation and the activation energy (ΔE) of gelation for the DTAx16 system differed significantly from those for the neat system. The times to gelation were decreased by the pre-

sence of the ATBN rubber, especially at low temperatures. The activation energy of gelation for the DTAx16 system was found to be 10.2 kcal/mole compared to 14.1 kcal/mole for the neat system, and 14.2 kcal/mole for the DTK-293 system. Furthermore, values of $_ET_{g\infty}$ for the DTAx16 system were sensitive to the conditions of cure as is indicated by the wide shaded band in the TTT diagram. The results of light transmission experiments in relation to the times for gelation and vitrification for the DTAx16 system are shown in Figure 15. Most of the phase separation occurred well before gelation but, as was observed for the DTK-293 system, did not cease until after gelation.

The thermomechanical spectra obtained after prolonged cure at different isothermal temperatures (Figure 16) show four relaxation processes in the logarithmic decrement plots: a high temperature relaxation associated with $_ET_g$; a broad relaxation at about -40°C; a relaxation at about -50°C associated with $_RT_g$; and one below $_RT_g$. The values of $_ET_g$ and $_ET_{g\infty}$ versus T_{cure} are included in Figure 17 and Table II, together with data for the neat system. The values of $_ET_{g\infty}$ were found to range from 125°C when cured at 100°C to 148°C when cured at 200°C. In comparison, the value of $_ET_{g\infty}$ for the neat system was 167°C which was independent of the isothermal temperature of cure. To cause a reduction of $_ET_{g\infty}$ equivalent to 42°C (from 167 to 125°C) for the 100°C cured specimen would require the epoxy matrix to contain 10% of rubber by weight as estimated by the Fox equation (33). However, the initial formulation for the DTAx16 system only contained 9.7% of rubber by weight and yet the volume fraction of phase-separated rubber appeared to be very high (see later and Table III). This indicated that the large decrease of $_ET_{g\infty}$ for the DTAx16 system

could not be caused by the dissolved rubber alone. TEM micrographs of a 100°C cured specimen (Figure 18a) and a 200°C cured specimen (Figure 18b) showed that the 100°C cured specimen had a much higher volume fraction of dispersed phase (V_f) than the 200°C cured specimen (see Table III) despite the $_ET_{g\infty}$ for the former specimen being much lower. Furthermore, the volume fraction of the dispersed phase of the DTAx16 system (both 100 and 200°C) was measured to be higher than for the DTK-293 specimens, although the values of $_ET_{g\infty}$ for the former specimens were much lower than for the latter specimens.

It is recognized that certain aliphatic amines promote homopolymerization of epoxy resins (34) and in fact, DGEBA-type epoxy resin can be cured at room temperature with commercial ATBN rubber if more than 50 phr of ATBN rubber is used (13). In order to study the level of reactivity of ATBN rubber in the DTAx16 system in the absence of TMAB, 15 phr of the commercially available ATBN rubber was mixed with 100 phr of DER 331 at 50°C and the mixture was heated at 200°C for two hours. The T_g of the mixture increased by 62°C (from -12 to 50°C) as determined from TBA thermomechanical spectra obtained before and after cure. A sample of ATBN rubber with negligible residual AEP content (NH equivalent weight ~ 1900 gm, supplied by the B. F. Goodrich Chemical Co.) was also examined. The T_g of the mixture of 100 phr DER 331/15 phr residue-free ATBN rubber was found to increase by 23°C (from -12 to 11°C) after cure at 200°C for two hours. The chemistry of cure for the DTAx16 system is therefore more complex than that for the neat system. The latter is considered to involve a stoichiometric reaction between epoxy and NH end groups. In contrast, homopolymerization of DER 331, reactions between the NH

end groups of the ATBN and DER 331, AEP and DER 331, and TMAB and DER 331 can all occur competitively for the DTAx16 system. The differences in cure chemistry between the DTAx16 and neat systems were reflected in the reaction kinetics by the times of gelation (Figure 14) and the activation energies of gelation for the two systems. Epoxy networks formed by stoichiometric reaction of epoxy resin and tetrafunctional aromatic diamine are highly crosslinked; for example the DER 331/TMAB system gives a $_ET_{g\infty}$ of 167°C. In contrast, cure of epoxy resins through homopolymerization usually give rise to more loosely crosslinked epoxy networks with low values of $_ET_{g\infty}$; for example, $_ET_{g\infty} \approx$ 100°C for a (5 phr) piperidine cured DGEBA-type epoxy system (5,34). Therefore, the large decrease of $_ET_{g\infty}$ for the DTAx16 system may reflect the extent of homopolymerization rather than the amount of dissolved rubber. To isolate the influence of homopolymerization on $_ET_{g\infty}$ in the absence of rubber, the values of $_ET_{g\infty}$ versus T_{cure} for a formulation of DER 331/TMAB/0.76 phr of AEP were obtained (AEP supplied by Aldrich Chemical Co.). In the formulation, the NH contribution from the AEP was made equivalent to the NH contribution from the commercial ATBN rubber (including its residual AEP) in the DTAx16 system. The values of $_ET_{g\infty}$ for the DER 331/TMAB/AEP formulation obtained by TBA experiments are presented in Figure 19, in which the data for the DTAx16 and neat systems are included for comparison. As for the DTAx16 system, values of $_ET_{g\infty}$ for the DER 331/TMAB/AEP formulation were also found to be dependent on T_{cure}, and ranged from 137°C when cured at 100°C to 161°C when cured at 200°C. At low T_{cure}, the reactivity of TMAB is low and so significant amounts of DER 331 epoxy could have homopolymerized before reacting with

TMAB to give rise to a low $_ET_{g\infty}$. At high T_{cure}, TMAB is more reactive and therefore the one-to-one reaction of epoxy with amine hydrogen would be expected to occur more competitively. A consequence of homopolymerization of epoxy in the DTAx16 system is the exclusion of amine hydrogen of TMAB from reaction, which will have deleterious effects on the physical properties.

It could be argued that the variation of $_ET_{g\infty}$ with T_{cure} for the DTAx16 system is caused by vaporization of AEP from the TBA specimens which increases with increasing temperature. However, values of $_ET_{g\infty}$ obtained from specimens (16), which had been machined from the large casting prepared in a sealed mold, were the same as those obtained from the TBA experiments. This suggests that the dependence of $_ET_{g\infty}$ on T_{cure} for the DTAx16 system results from the competing reactions during cure. A study of a DGEBA-type epoxy resin cured with a stoichiometric amount of AEP also concluded that the cure mechanism varied with cure conditions (35).

TEM micrographs of the 100 and 200°C cured specimens (Figure 18) show that the boundaries of the dispersed phase of the DTAx16 specimens were not as well-defined as those in the DTK-293 specimens. Similar results have also been reported elsewhere (36). The values of the volume fractions (V_f) of dispersed phase for the two specimens determined by both Schwartz-Saltykov's diameter (22) and Spektor's chord (22) methods were similar (Table III); the value of V_f for the 100°C cured specimen ($V_f \sim 0.34$) was much higher than that for the 200°C cured specimen ($V_f \sim 0.15$). Both methods revealed that the two specimens displayed a unimodal distribution of particle size; and that the 200°C cured specimen has a higher percentage of smaller particles but a wider

range of particle sizes. The size distributions of the two specimens obtained by using Schwartz-Saltykov's diameter method are shown in Figure 20. The apparent differences of the values of mean diameter (d) of the particles for the 200°C cured specimen determined by the two methods (Table III) may be a consequence of the underestimation of the percentage of smaller particles in this specimen when using the Spektor's method (as discussed previously for the DTK-293 200°C cured specimen).

The high volume fraction of dispersed phase for the 100°C specimen ($V_f \sim$ 0.34) indicates that a large amount of epoxy was present in the dispersed phase since the initial volume fraction of rubber added was approximately 0.11. This is probably a result of initiation of epoxy homopolymerization by the rubber. The 100°C cured specimen is a translucent casting whereas the 200°C cured specimen is an opaque solid resembling the rubber-modified DTK-293 specimens. The translucency is also probably a consequence of the large amount of epoxy in the dispersed phase for the 100°C cured specimen, the inclusions having a refractive index not very different from the surrounding epoxy matrix. Since the increasing relative amounts of epoxy in the domains is not accompanied by an increase in the temperature of $_RT_g$ (Figure 16), epoxy and rubber are not in solution in the domains. An SEM micrograph of the fracture surfaces for the 100°C cured specimen (Figure 21) shows a characteristic texture inside the boundaries of the domains. In contrast, SEM micrographs of the fracture surfaceds for the 200°C cured specimen and the DTK-293 (100 and 200°C) specimens (16), as well as for other similar rubber-modified epoxy specimens (6,7), generally show "holes" for the sites of the dispersed phase (7).

CONCLUSIONS

The effect of cure conditions on the transitions and morphology for two rubber-modified epoxy systems has been investigated using torsional braid analysis (TBA), light transmission, and electron microscopy. Time-temperature-transformation (TTT) isothermal cure diagrams and plots of the subsequent glass transition temperatures versus the temperatures of cure were used as a basis for comparing the cure behavior and structure-property relationships for the neat and the two rubber-modified systems. During cure, most of the rubber phase-separated well before gelation. Of the two rubber-modified systems, the volume fraction of the dispersed phase and the values of the maximum glass transition temperatures ($_E T_{g\infty}$) for the amino-terminated rubber-modified system were found to be more se-stive to cure conditions than was the prereacted carboxyl-terminated rubber-modified system. The values of $_E T_{g\infty}$ for the systems were in the order: neat (167°C) > prereacted carboxyl-terminated (161 to 163°C) > amino-terminated (125 to 148°C). Unlike the amino-terminated rubber-modified system, the chemistry of cure for the prereacted carboxyl-terminated rubber-modified and neat systems is essentially the same which accounts for the similarity of the reaction kinetics as measured by the times to gelation and the activation energies of gelation. The relatively small decrease of $_E T_{g\infty}$ for the prereacted carboxyl-terminated rubber-modified system was attributed to dissolved rubber. In contrast, dissolved rubber cannot account for the large decrease of $_E T_{g\infty}$ for the amino-terminated rubber-modified system, which also has the highest volume fraction of dispersed

phase. The anomaly for the amino-terminated rubber-modified system was attributed to the complexity of the cure chemistry which was introduced by using the rubber.

ACKNOWLEDGMENTS

LITERATURE CITED

1. McGarry, F. J.; Willner, A. M. "Toughening of an Epoxy Resin by An Elastomeric Second Phase"; Massachusetts Institute of Technology: Cambridge, 1968; Research Report R68-8.

2. Sultan, T. N.; McGarry, F. J. Polym. Engr. Sci. 1973, 13, 29.

3. Riew, C. K.; Rowe, E. H.; Siebert, A. R. in "Toughness and Brittleness of Plastics"; Deanin, R. D.; Crugnola, A. M., Eds.; ADVANCES IN CHEMISTRY SERIES No. 154, American Chemical Society: Washington, D.C., 1976; p. 326.

4. Bucknall, C. B.; Yoshii, T., Br. Polym. J. 1978, 10, 53.

5. Manzione, L. T.; Gillham, J. K.; McPherson, C. A. J. Appl. Polym. Sci. 1981, 26, 889.

6. Manzione, L. T.; Gillham, J. K.; McPherson, C. A. J. Appl. Polym. Sci. 1981, 26, 907.

7. Kinloch, A. J.; Shaw, S. J.; Tod, D. A.; Hunston, D. L. Polymer 1983, 24, 1341.

8. Kinloch, A. J.; Shaw, S. J.; Hunston, D. L. Polymer 1983, 24, 1355.

9. Kunz-Douglass, S.; Beaumont, P. W. R.; Ashby, M. F. J. Mater. Sci. 1980, 15, 1109.

10. Sayre, J. A.; Kunz, S. C.; Assink, R. A. Polymer Prepr., Am. Chem. Soc., Div. Polym. Mat.: Sci. Engr. 1983, 49, 442.

11. Bascom, W. D.; Cottington, R. L.; Jones, R. L., Peyser, P. J. Appl. Polym. Sci. 1975, 19, 2545.

12. Laible, R. C.; McGarry, F. J. Polym. Plast. Tech. Engr. 1976, 7, 27.

13. Riew, C. K. Rubber Chem. Tech. 1981, 54, 374.

14. Gillham, J. K., in "The Role of the Polymeric Matrix in the Processing and Structural Properties of Composite Materials"; Seferis, J. C.; Nicolais, L., Eds.; Plenum Press: New York, 1983; p. 127.

15. Williams, R. J. J.; Borrajo, J.; Adabbo, H. E.; Rojas, A. J. Polym. Prepr., Am. Chem. Soc., Div. Polym. Mat.: Sci. Engr. 1983, 49, 432.

16. Chan, L. C.; Gillham, J. K.; Kinloch, A. J.; Shaw, S. J. in "Rubber-Modified Thermoset Resins"; Riew, C. K.; Gillham, J. K., Eds.; ADVANCES IN CHEMISTRY SERIES NO. 209, American Chemical Society: Washington, D.C., 1984; p. XXX.

17. Chan, L. C.; Gillham, J. K. Polym. Prepr., Am. Chem. Soc., Div. Polym. Mat.: Sci. Engr. 1983, 48, 571.

18. "Mold Preparation for Araldite Resins, Instruction Manual", Ciba-Geigy Chem. Co., 1972.

19. Gillham, J. K., in "Developments in Polymer Characterisation-3"; Dawkins, J. V., Ed.; Applied Science Publishers: London, 1982; p. 159.

20. Enns, J. B.; Gillham, J. K. in "Computer Applications in Applied Polymer Science"; Provder, T., Ed.; ADVANCES IN CHEMISTRY SERIES No. 197, American Chemical Society: Washington, D.C., 1982; p. 329.

21. Deguchi, T. J. M.Sci. Thesis, Princeton University, New Jersey, 1983.

22. Underwood, E. E., in "Quantitative Microscopy", DeHoff, R. T.; Rhines, F. N., Eds.; McGraw-Hill: New York, 1968; Chap. 6.

23. Enns, J. B.; Gillham, J. K. J. Appl. Polym. Sci. 1983, 28, 2567.

24. "High-Performance, Low-Energy-Curing Resins", National Materials Advisory Board, National Research Council, Publication NMAB-412, National Academy Press, Washington, D.C., 1984.

25. Pogany, G. A. Polymer 1970, 11, 66.

26. Naé, H. N.; Gillham, J. K. Polym. Prepr., Am. Chem. Soc., Div. Org. Coat. Plast. Chem., 1983, 48, 566.

27. Enns, J. B.; Gillham, J. K. in "Polymer Characterization: Spectroscopic, Chromatographic, and Physical Instrumental Methods"; Craver, C. D., Ed.; ADVANCES IN CHEMISTRY SERIES No. 203, American Chemical Society: Washington, D.C., 1983; p. 27.

28. Enns, J. B.; Gillham, J. K. J. Appl. Polym. Sci. 1983, 28, 2831.

29. Shimazaki, A. J. Polym. Sci., Part C 1968, 23, 555.

30. Visconti, S.; Marchessault, R. H. Macromolecules 1974, 7, 913.

31. Wang, T. T.; Zupko, H. M. J. Appl. Polym. Sci. 1981, 26, 2391.

32. Keskkula, H.; Turley, S. G.; Boyer, R. F. J. Appl. Polym. Sci. 1971, 15, 351.

33. Fox, T. G. Bull. Am. Phys. Soc. 1956, 1, 123.

34. Lee, H.; Neville, K. "Handbook of Epoxy Resins"; McGraw Hill: New York, 1967.

35. Osinski, J. S.; Manzione, L. T. in "Epoxy Resin Chemistry II"; Bauer, R. S., Ed.; ACS SYMPOSIUM SERIES No. 221, American Chemical Society: Washington, D.C., 1983; p. 263.

36. Kunz, S. C.; Sayre, J. A.; Assink, R. A. Polymer 1982, 23, 1897.

TABLE CAPTIONS

I. Chemical Formulations of the Neat, DTK-293 and DTAx16 Systems.

II. Glass Transition Temperatures Versus T_{cure} for the Neat, DTK-293 and DTAx16 Systems.

III. Effect of Cure Conditions on Morphology for the DTK-293 and DTAx16 Systems.

FIGURE CAPTIONS

1. Chemical Structures of the Reactants.

2. Representative TBA Isothermal Cure Spectra for the Neat System (DER 331/TMAB): Relative Rigidity (a) and Logarithmic Decrement (b) vs. Time.

3. TTT Isothermal Cure Diagram for the Neat System (DER 331/TMAB): (+) gelation; (o) vitrification.

4. Representative TBA Thermomechanical Spectra after Isothermal Cure for the Neat System (DER 331/TMAB): Relative Rigidity (a) and Logarithmic Decrement (b) vs. Temperature.

5. $_E T_g$, $_E T_{g\infty}$, $_E T_{sec}$ and $_E T_{sec\infty}$ vs. T_{cure} for the Neat System (DER 331/TMAB):

   ($\square$) $_E T_g$; (+) $_E T_{g\infty}$; (o) $_E T_{sec}$; ($\lozenge$) $_E T_{sec\infty}$.

6. Representative TBA Isothermal Cure Spectra for the Rubber-modified DTK-293 System: Relative Rigidity (a) and Logarithmic Decrement (b) vs. Time.

7. TTT Isothermal Cure Diagram (Rubber-Modified DTK-293 System vs. Neat System): ($\square$) gelation (DTK-293); (*) vitrification (DTK-293); (+) gelation (neat); (o) vitrification (neat).

8. TTT Isothermal Cure Diagram Including Phase-Separation for the Rubber-Modified DTK-293 System: ($\square$) gelation; (*) vitrification; (+)

cloud point; (Δ) 90% decrease of light intensity; ( ) end of phase-
separation.

9. Representative TBA Thermomechanical Spectra after Isothermal Cure for
    the Rubber-Modified DTK-293 System: Relative Rigidity (a) and
    Logarithmic Decrement (b) vs. Temperature.

10. $_E T_g$ and $_E T_{g\infty}$ vs. T_{cure} (Rubber-Modified DTK-293 System and Neat System):
    (*) $_E T_g$ (DTK-293); ($\square$) $_E T_{g\infty}$ (DTK-293); (o) $_E T_g$ (Neat); ($\Diamond$) $_E T_{g\infty}$ (Neat).

11. TEM Micrographs for Cured Rubber-Modified DTK-293 Specimens: a) T_{cure}
    = 100°C, b) T_{cure} = 200°C.

12. Size Distributions of the Rubber-Modified DTK-293 100 and 200°C
    Cured Specimens from Analysis of TEM Micrographs using Schwaretz-
    Saltykov's Diameter Method.

13. Representative TBA Isothermal Cure Spectra for the Rubber-Modified
    DTAx16 System: Relative Rigidity (a) and Logarithmic Decrement (b) vs.
    Time.

14. TTT Isothermal Cure Diagram (Rubber-Modified DTAx16 System vs. Neat
    System): ($\square$) gelation (DTAx16); (*) vitrification (DTAx16); (+) gela-
    tion (neat); (o) vitrification (neat).

15. TTT Isothermal Cure Diagram Including Phase-Separation for the Rubber-
    Modified DTAx16 System: ($\square$) gelation; (*) vitrification; (+) cloud
    point; (Δ) 90% decrease of light intensity; ($\Diamond$) end of phase-separa-
    tion.

16.   Representative TBA Thermomechanical Spectra after Isothermal Cure for the Rubber-Modified DTAx16 System: Relative Rigidity (a) and Logarithmic Decrement (b) vs. Temperature.

17. $_ET_g$ and $_ET_{g\infty}$ vs. T_{cure} (Rubber-Modified DTAx16 System and Neat System): (*) $_ET_g$ (DTAx16); (▭) $_ET_{g\infty}$ (DTAx16); (O) $_ET_g$ (neat); (◊) $_ET_{g\infty}$ (Neat).

18.   TEM Micrographs for Cured Rubber-Modified DTAx16 Specimens: a) T_{cure} = 100°C, b) T_{cure} = 200°C.

19. $_ET_{g\infty}$ vs. T_{cure} (DER 331/TMAB/AEP, Rubber-Modified DTAx16 System and Neat System): (◊) neat; (o) DER 331/TMAB/AEP; (▢) DTAx16

20.   Size Distributions of the Rubber-Modified DTAx16 100 and 200°C Cured Specimens from Analysis of TEM Micrographs using Schwartz-Saltykov's Diamete Method.

21.   SEM Micrograph of a 100°C Cured Rubber-Modified DTAx16 Specimen. (Fracture Temperature = -20°C).

TABLE I. Chemical Formulations of the Neat, and the Rubber-Modified
DTK-293 and DTAx16 Systems.

	Neat	DTK-293	DTAx16
DER 331	100.0	100.0	100.0
TMAB	41.0	51.0	39.9
K-293	-	42.0	-
ATBNx16	-	-	15.0

The basis for the formulations is as follows:
a) Neat System (no rubber): 1 epoxy/1 amine hydrogen
b) Rubber-Modified Systems: i) 15 phr of rubber based on
     100 phr of unreacted epoxy; ii) 1 free epoxy/1 amine
     hydrogen: assuming all epoxy end groups in DTK-293
     (from the rubber-containing chains and the DGEBA resin)
     and in DER 331 react with TMAB; and assuming all NH in
     ATBN rubber (including NH in AEP) and TEM react with
     epoxy.
The initial volume fractions of rubber (V_0) in the two
rubber-modified formulations are about the same ($V_0 \sim 0.11$).

TABLE II. Glass Transition Temperatures Versus
Cure Temperature (TBA Data)

T_{cure}/Time ($^\circ$C) /(hr)	Neat		DTK-293		DTAx16	
	$_E T_g$ (Hz)	$_E T_{g\infty}$ (Hz)	$_E T_g$ (Hz)	$_E T_{g\infty}$ (Hz)	$_E T_g$ (Hz)	$_E T_{g\infty}$ (Hz)
100 / 40	124 (0.5)	166 (0.6)	122 (0.5)	163 (0.5)	120 (0.5)	125 (0.6)
120 / 36	142 (0.5)	167 (0.5)	140 (0.5)	162 (0.5)	135 (0.5)	136 (0.5)
150 / 24	161 (0.6)	166 (0.6)	157 (0.5)	161 (0.6)	145 (0.6)	145 (0.6)
170 / 10	167 (0.6)	167 (0.6)	161 (0.5)	161 (0.5)	146 (0.6)	146 (0.6)
200 / 3	166 (0.6)	166 (0.6)	161 (0.5)	161 (0.5)	148 (0.6)	148 (0.6)

$_E T_g$ = glass transition temperature as cured, $^\circ$C.

$_E T_{g\infty}$ = maximum glass transition temperature after postcure, $^\circ$C.

TABLE III. Effect of Cure Conditions on Morphology

Cure Conditions	DTK-293			DTAx16		
T_{cure}/Time (hr)	d(μm)	V_f	V_f^*	d(μm)	V_f	V_f^*
100°C / 40	0.6	0.11	0.13	3.1	0.34	0
+170°C / 5	(0.6)	(0.11)		(2.7)	(0.38)	
200°C / 3	1.5	0.13	0.13	1.8	0.15	0.08
	(2.9)	(0.14)		(2.7)	(0.17)	

d = mean diameter of particles determined by Schwartz-Saltykov's diameter method (Spektor's chord method in brackets)

V_f = volume fraction of dispersed phase determined by Schwartz-Saltykov's diameter method (Spektor's chord method in brackets)

V_f^* = volume fraction of dispersed phase determined using the Fox equation (see text)

NEAT SYSTEM

EPOXY: Diglcidyl Ether of Bisphenol A (DER 331)
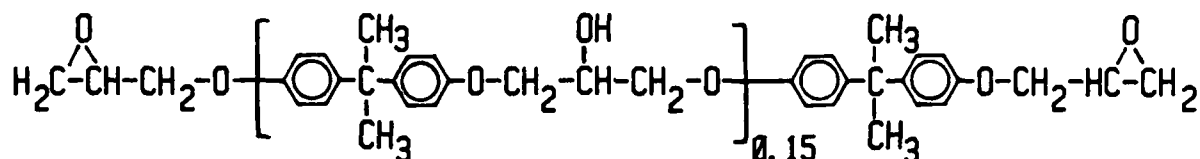
AMINE: Trimethylene Glycol Di-p-aminobenzoate (TMAB)
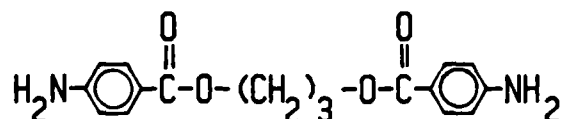
REACTIVE LIQUID RUBBER

i) Prereacted Carboxyl-Terminated Copolymer of Butadiene
and Acrylonitrile (AN content of rubber = 17 %) (K-293)

+ excess
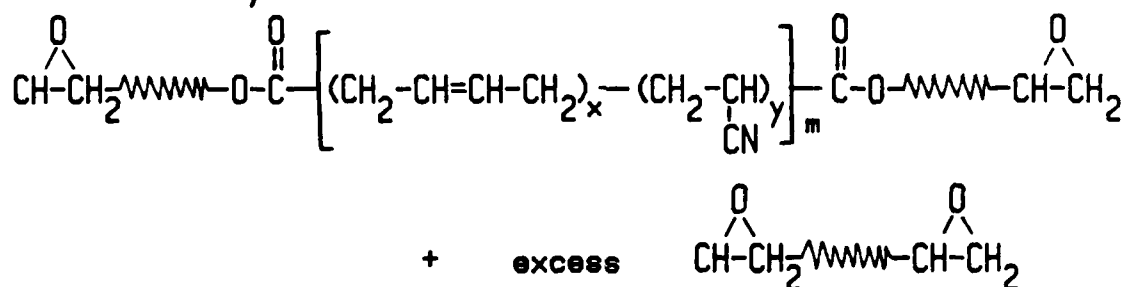
ii) Amino-Terminated Copolymer of Butadiene and Acrylonitrile
(AN content = 17 %) (ATBNx16)

+ 3 %
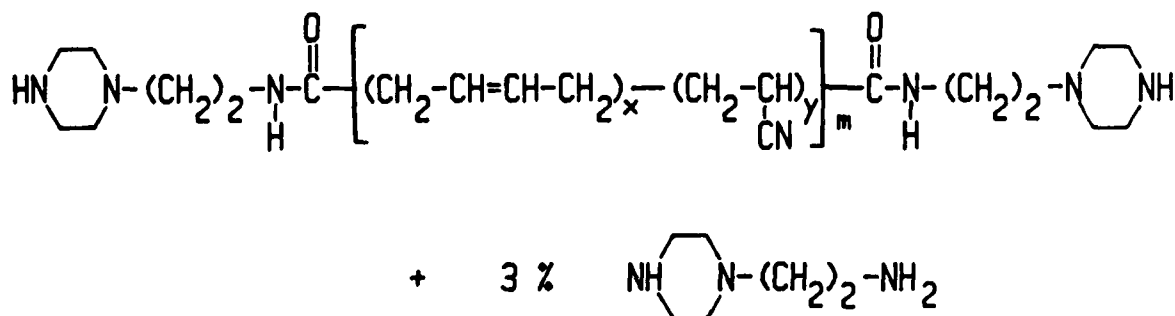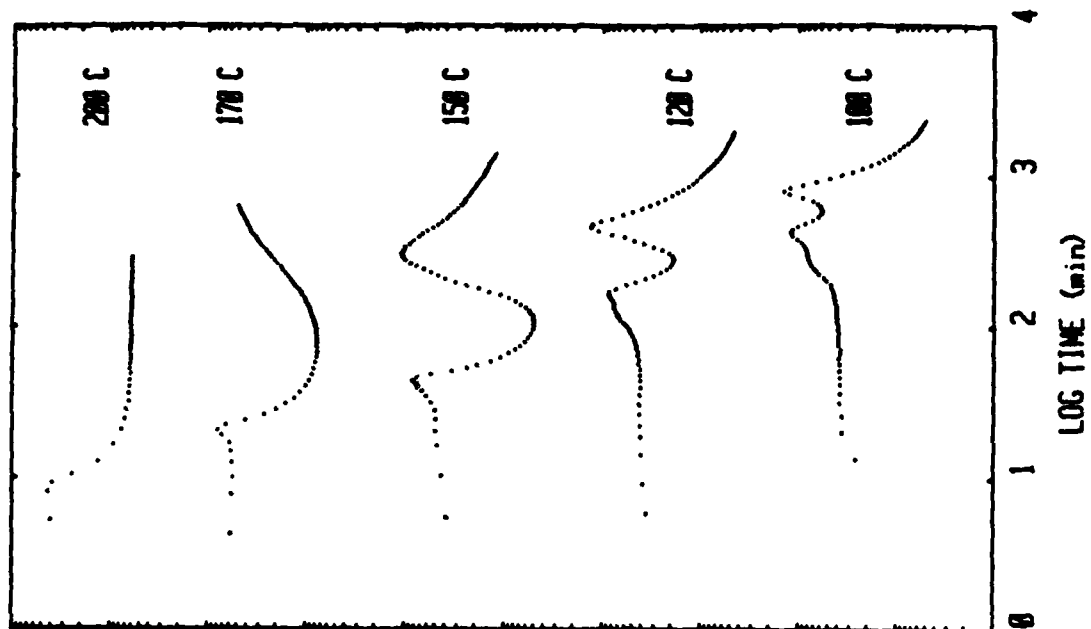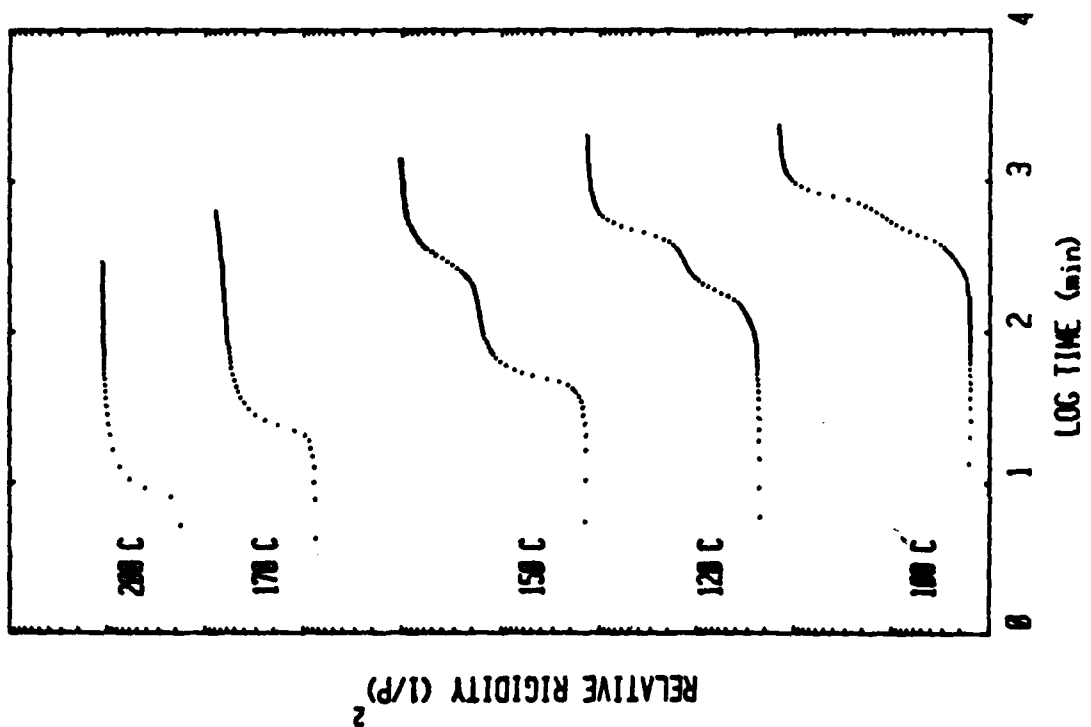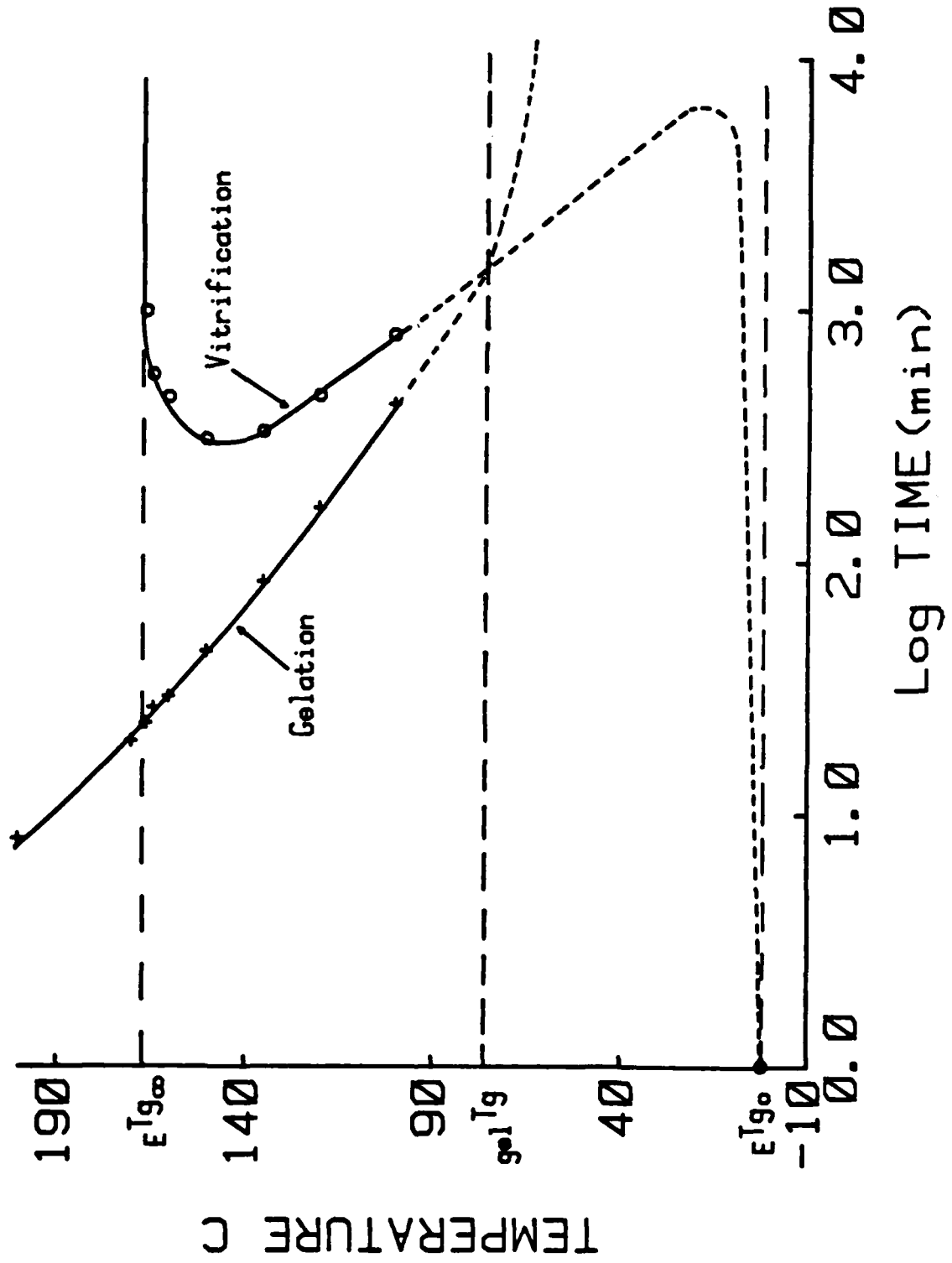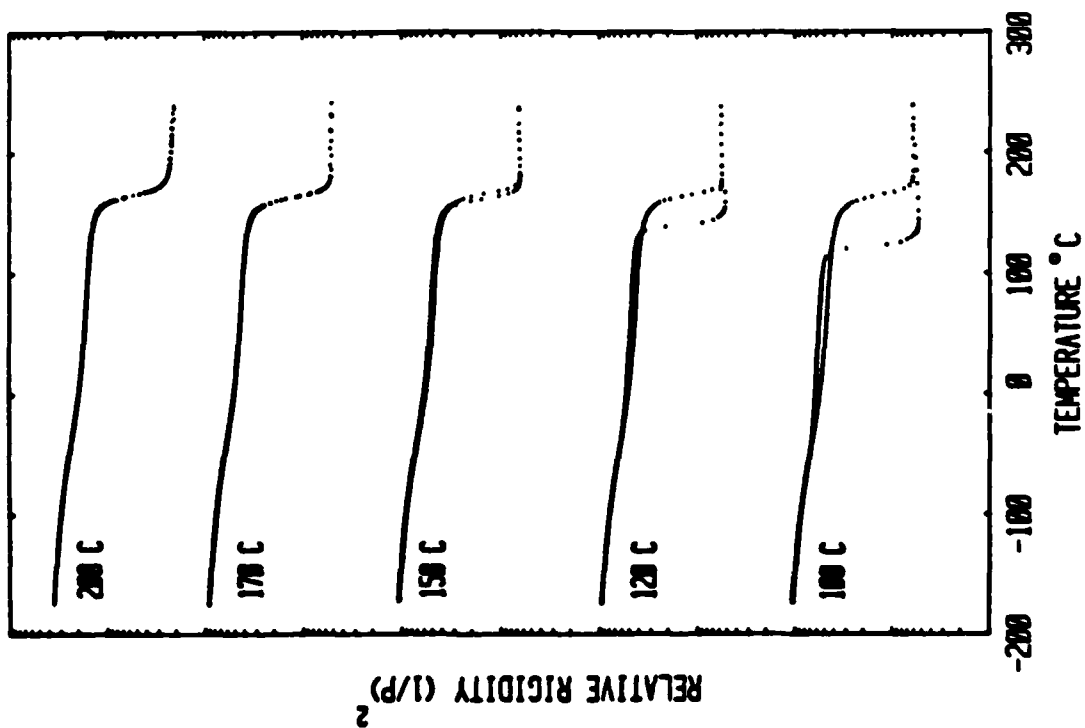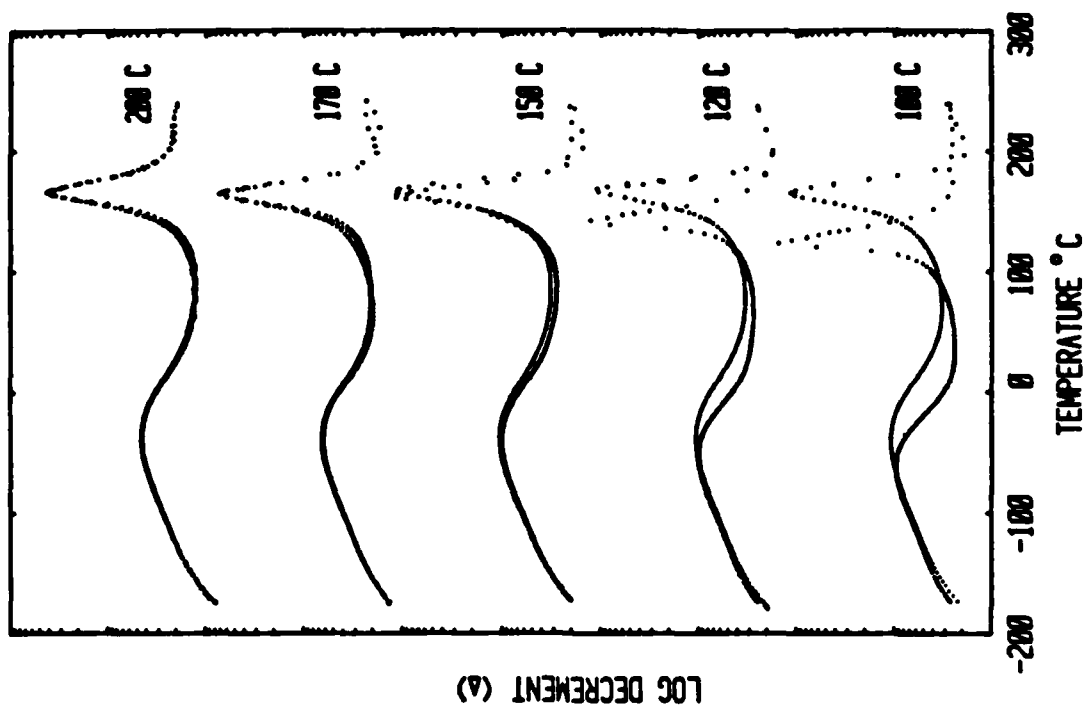
Figure 1

Figure 2

Figure 3

Figure 4
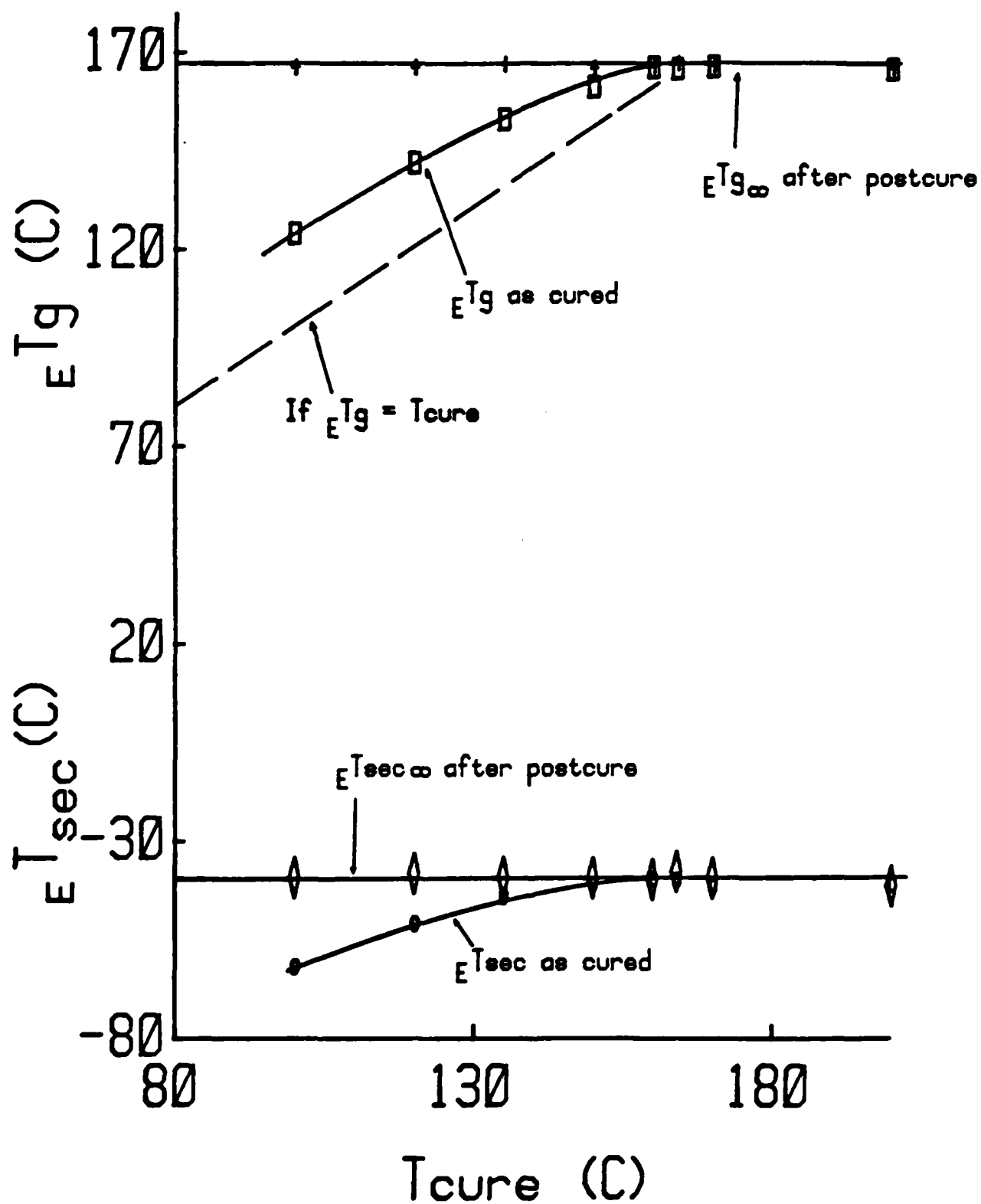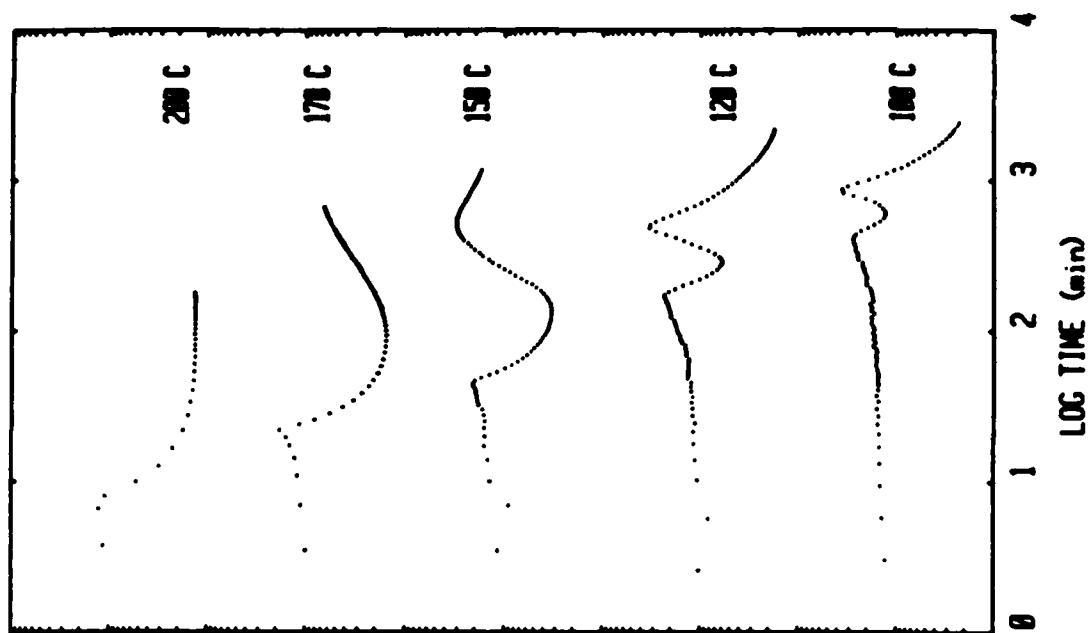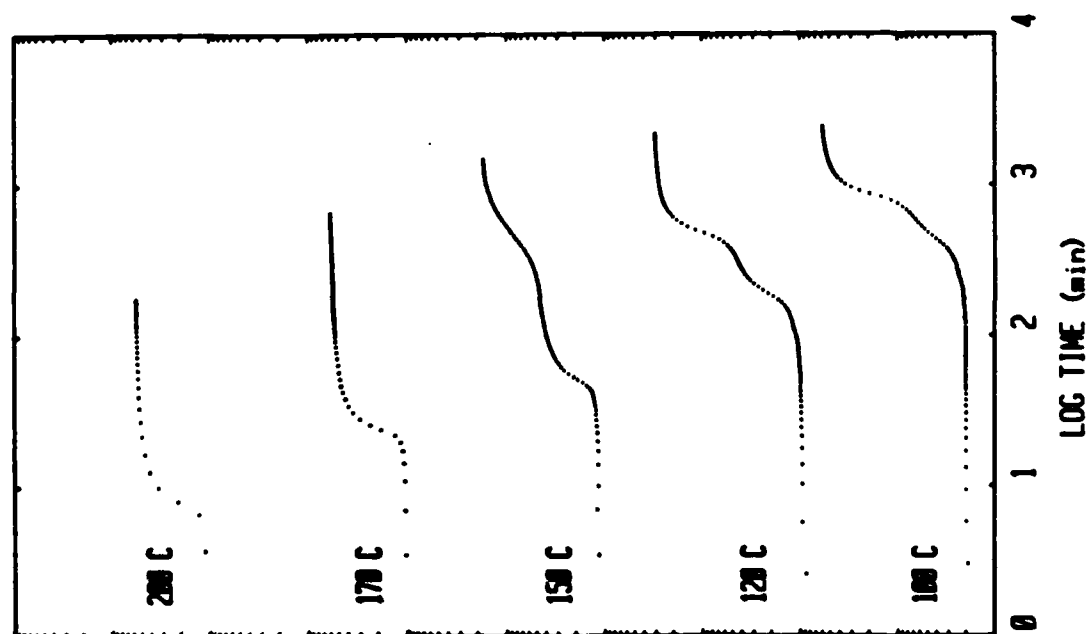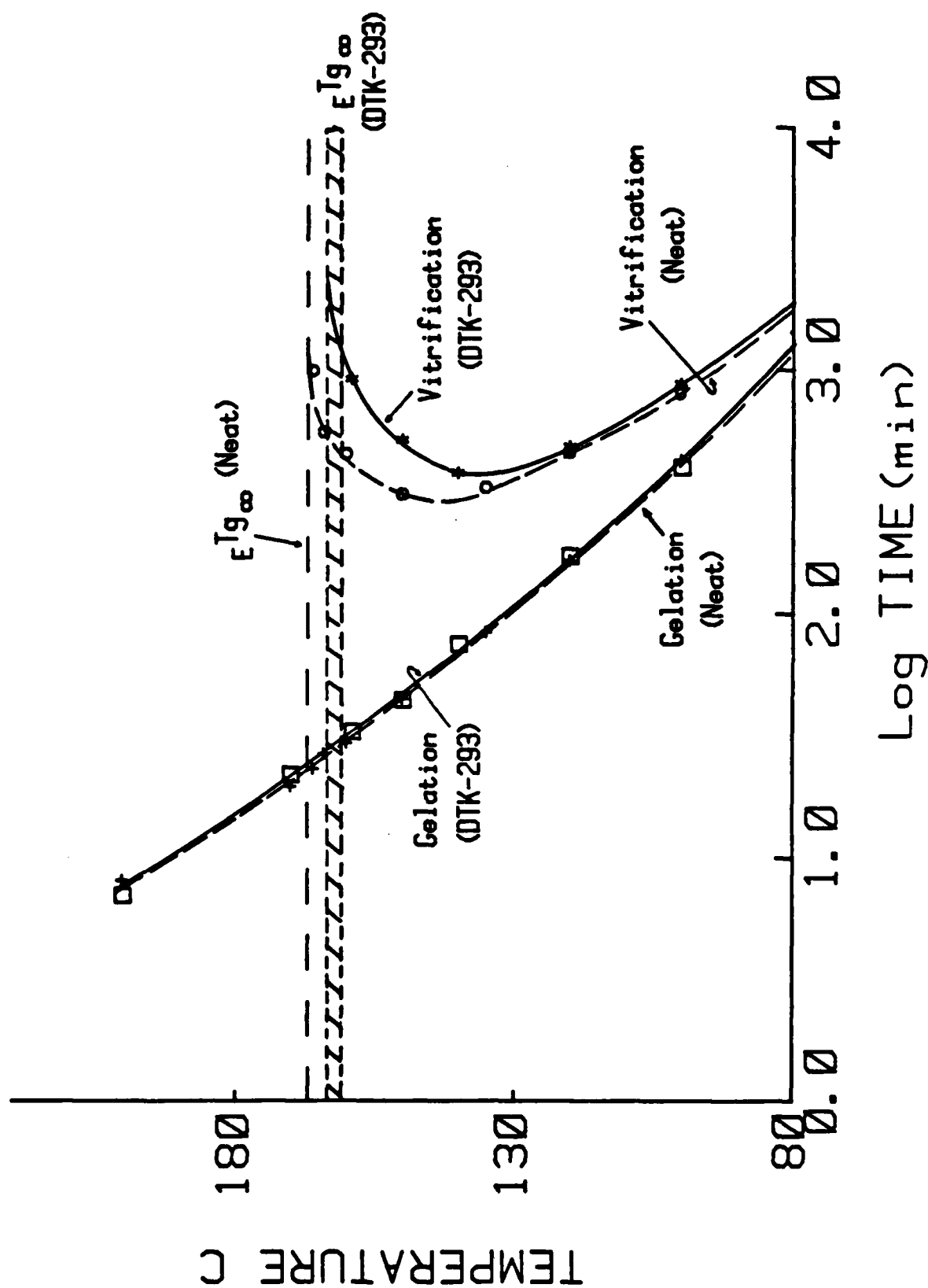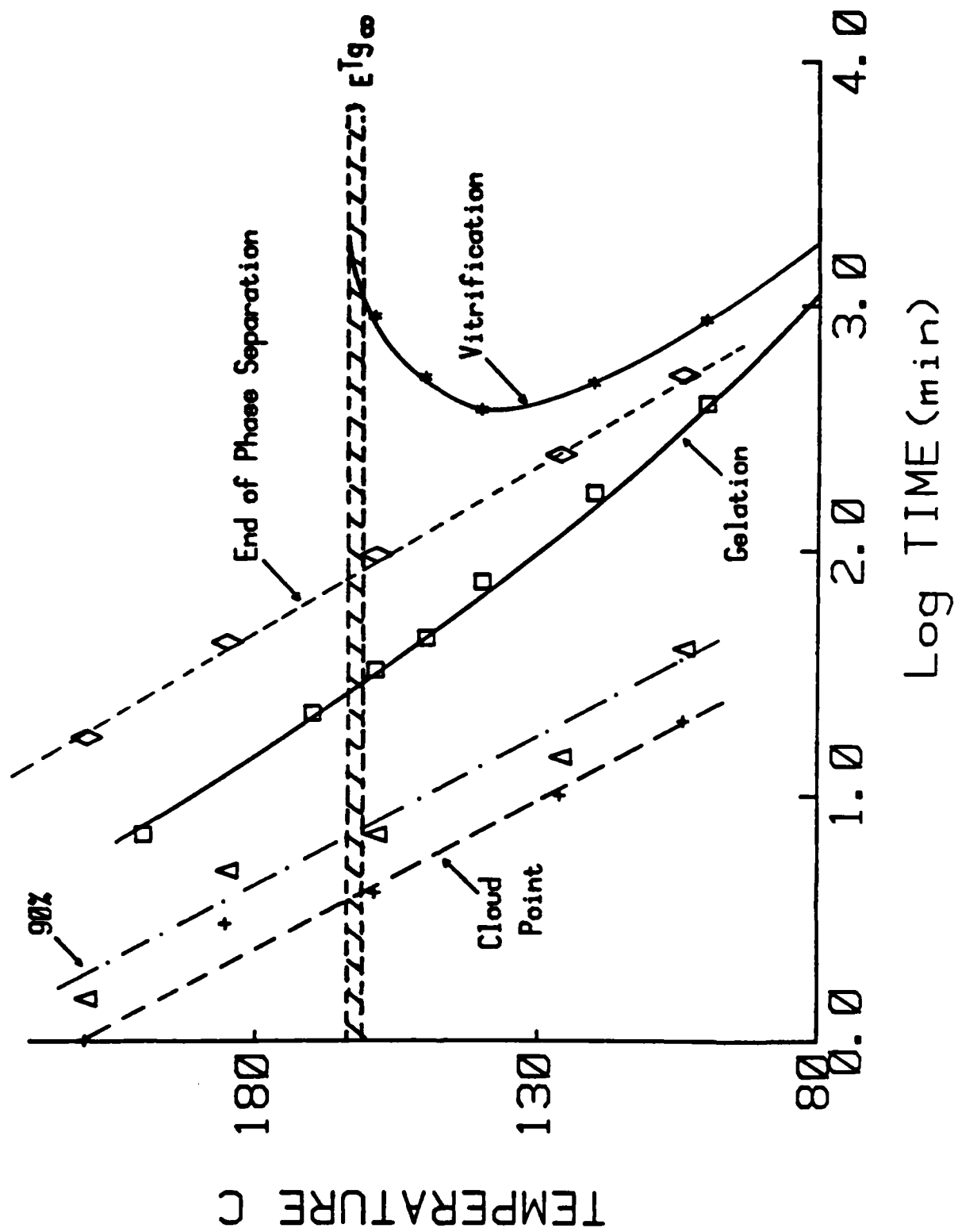
Figure 5

Figure 6

Figure 7

Figure 8
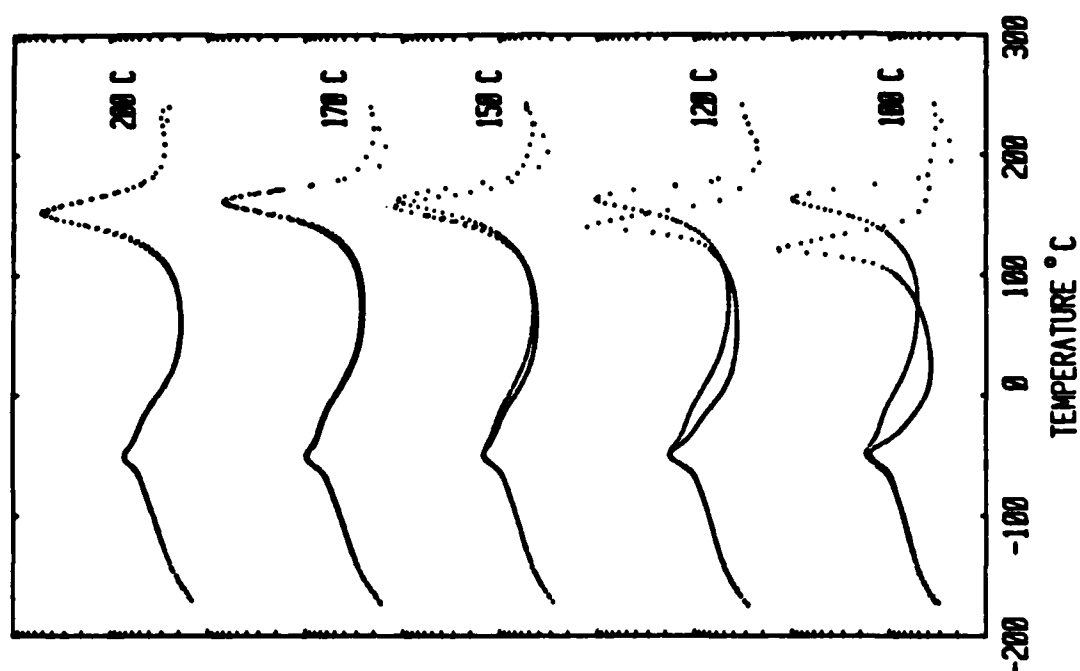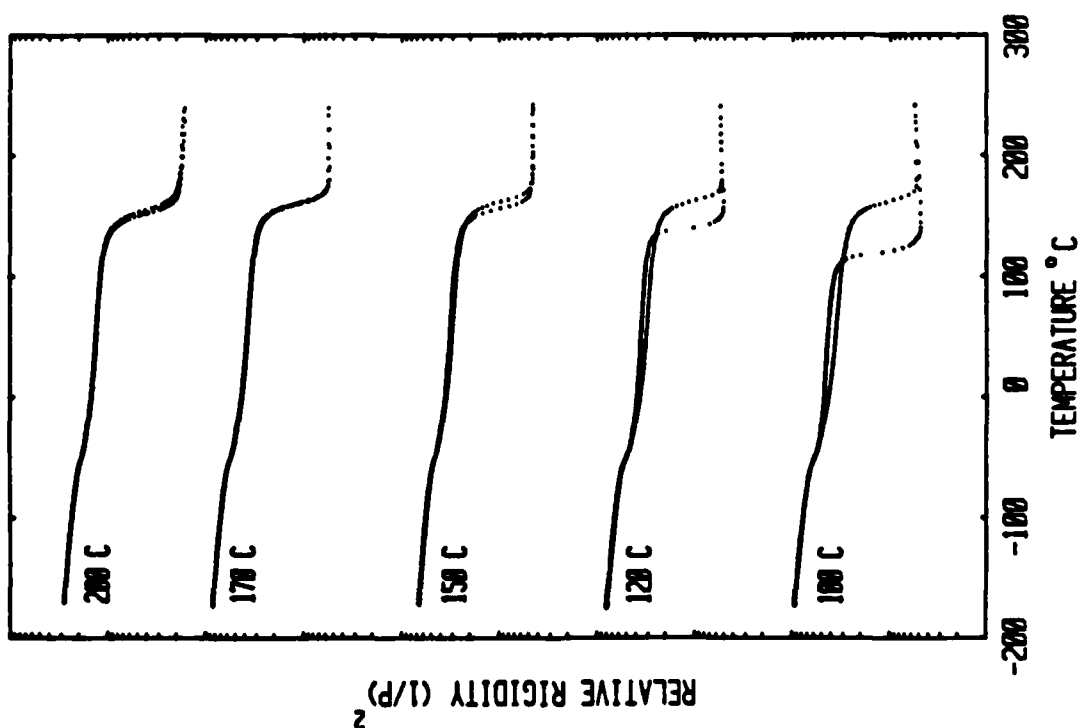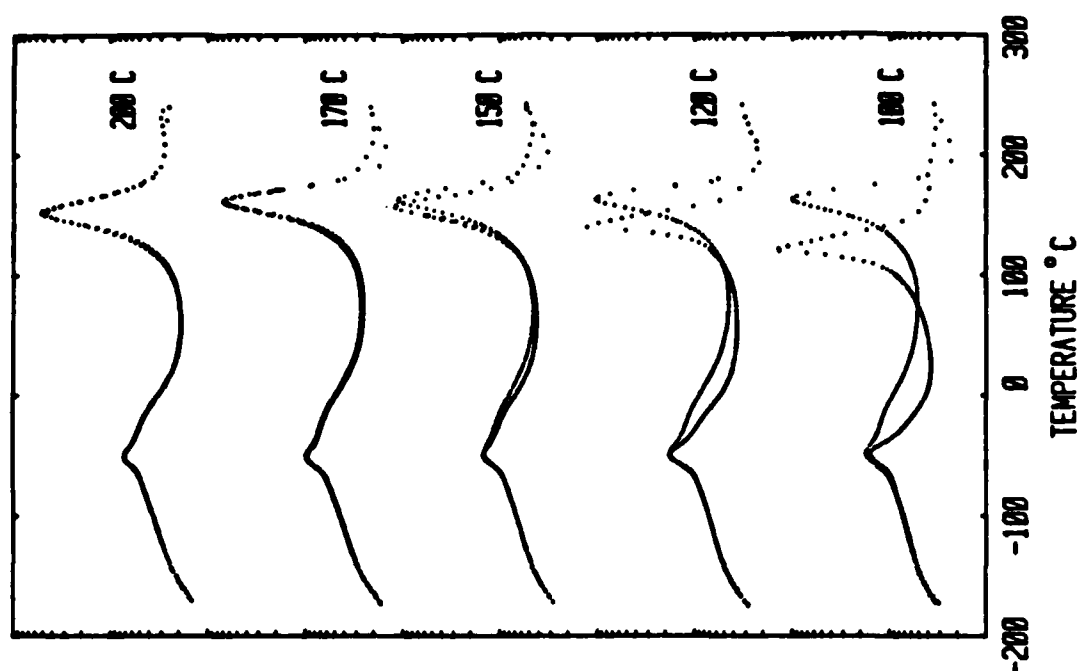
Figure 9

Figure 10

(a)

2 μm

Figure 11

2 μm

(b)
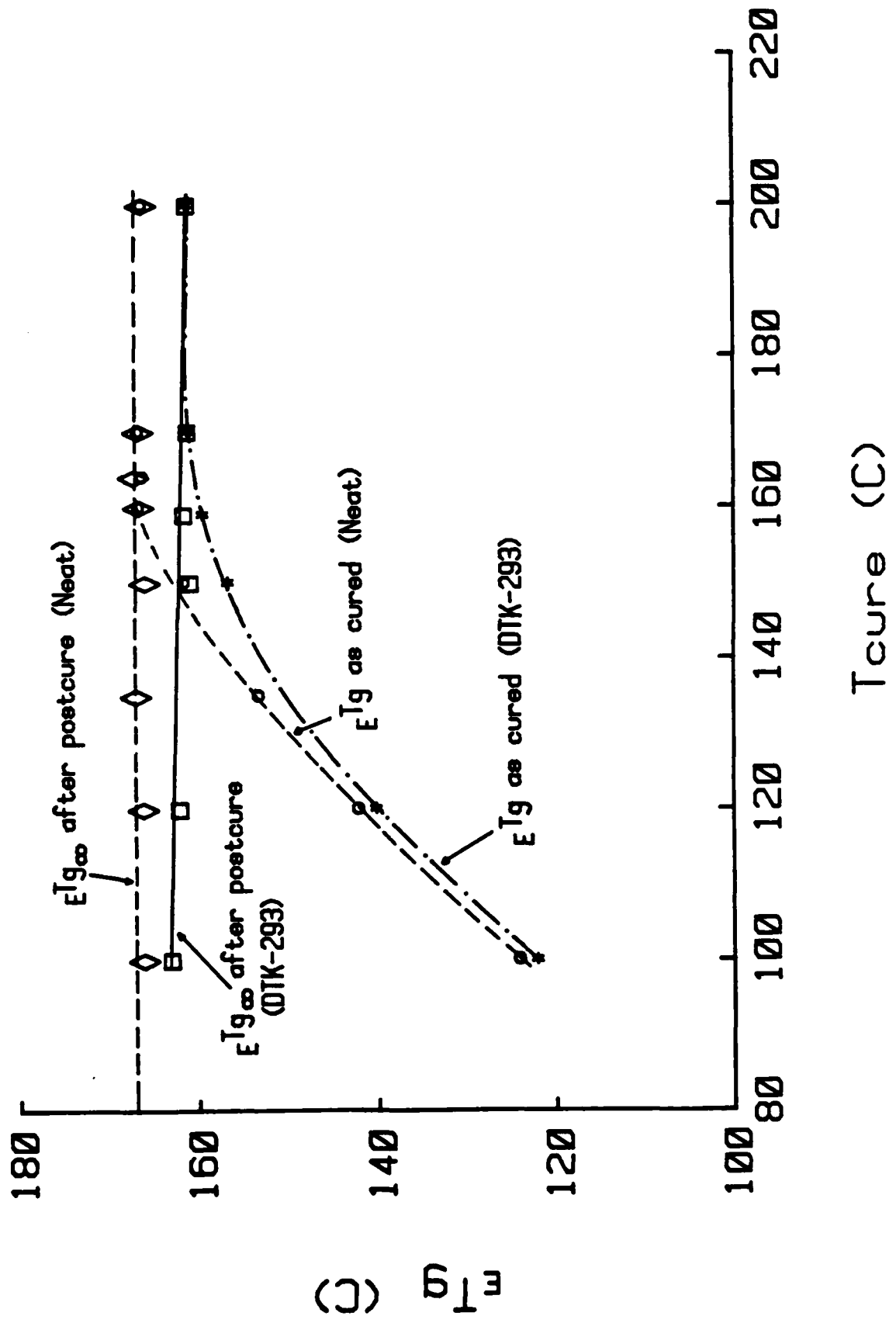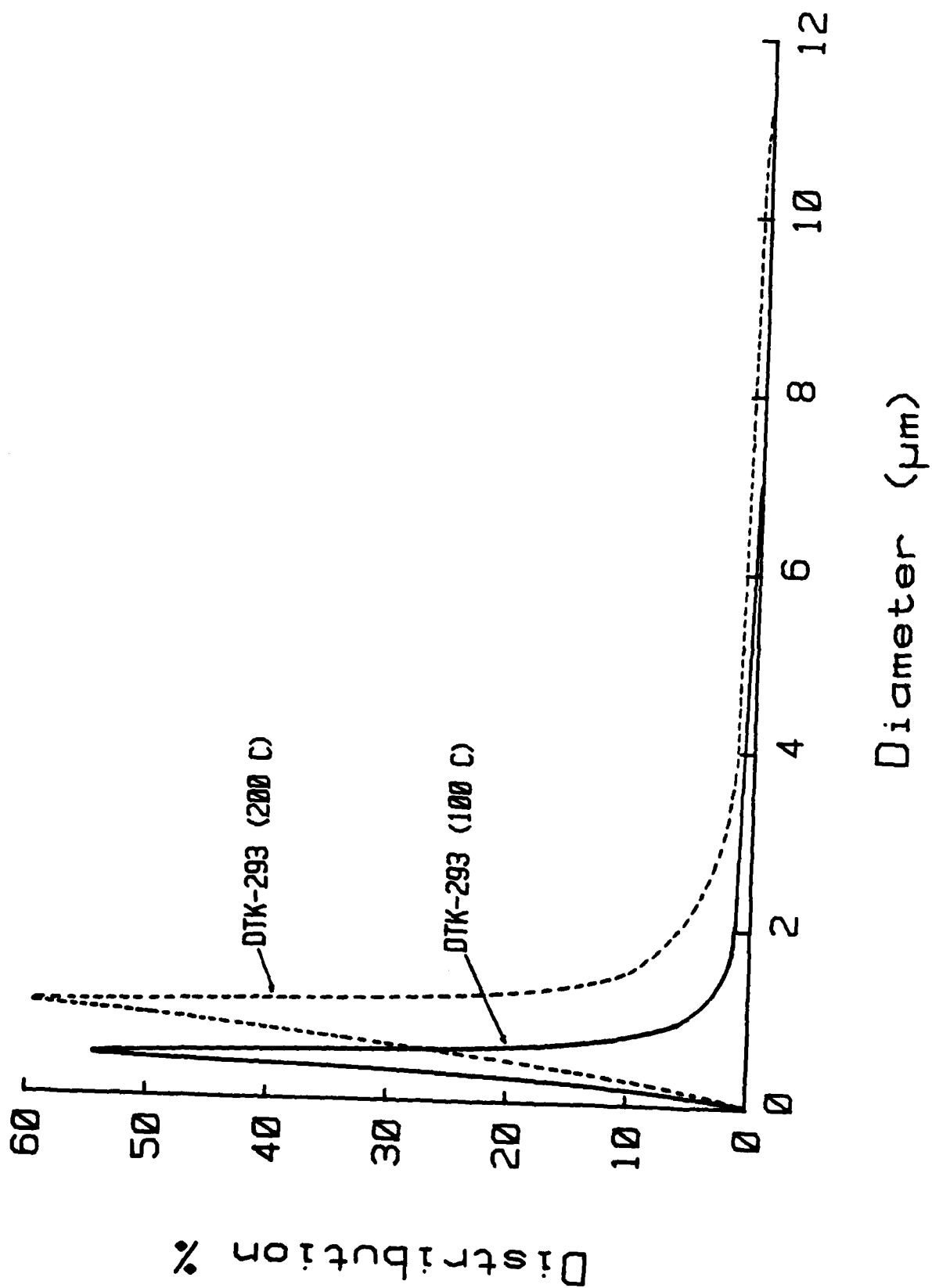
Figure 11

Fig. 12
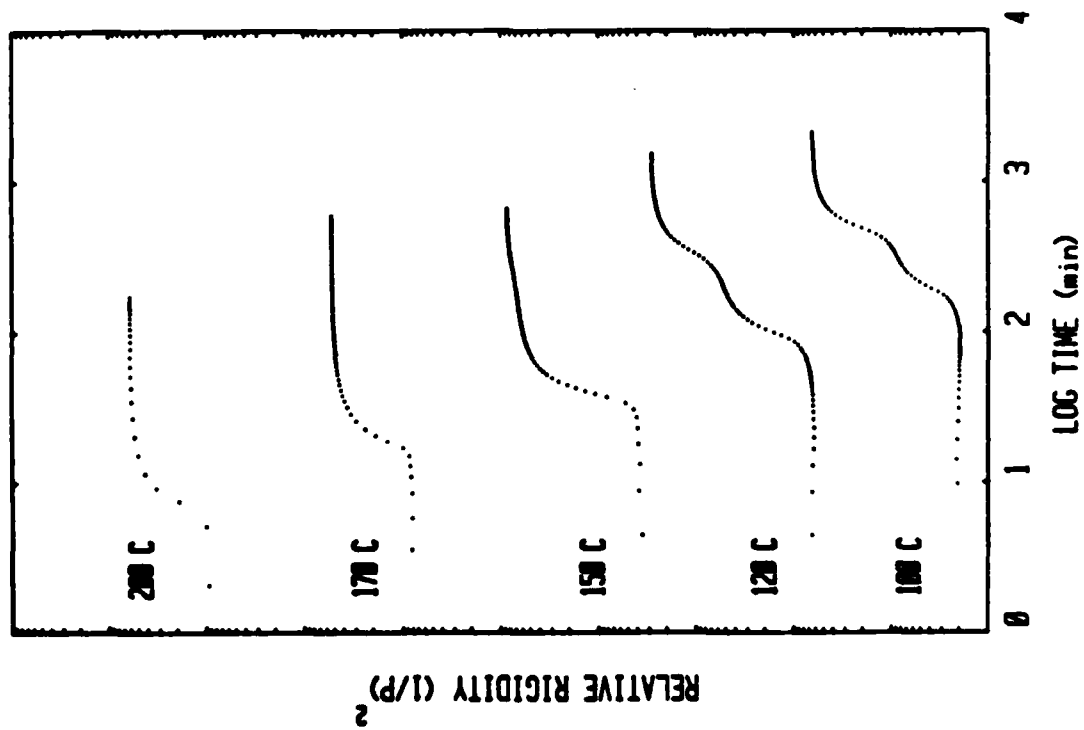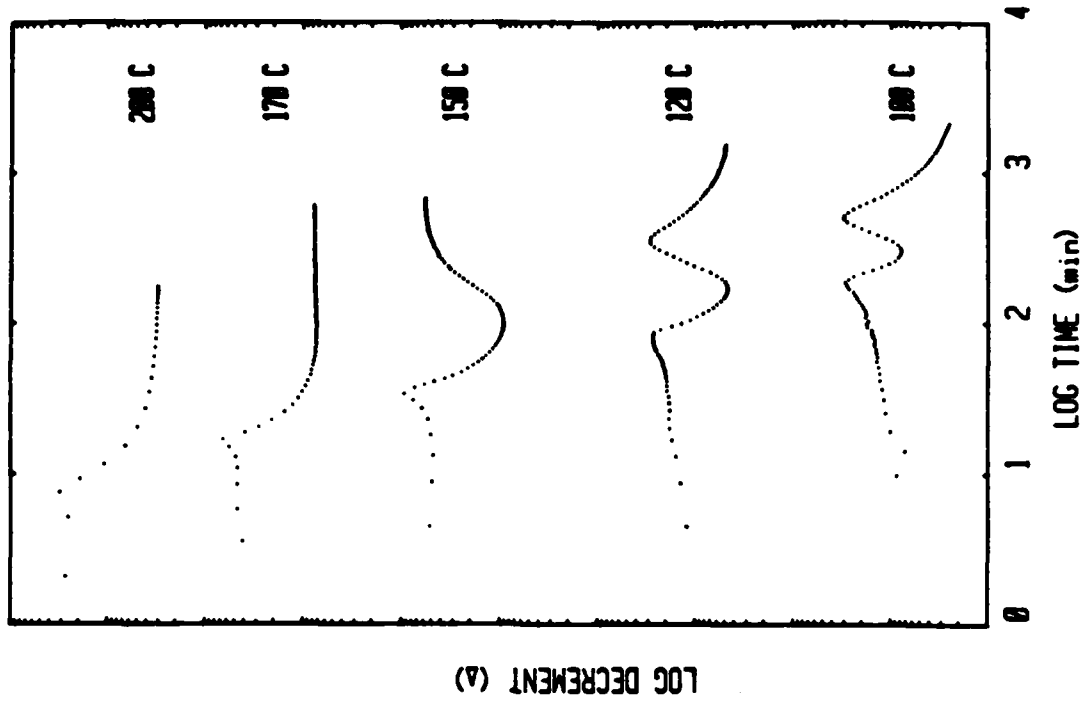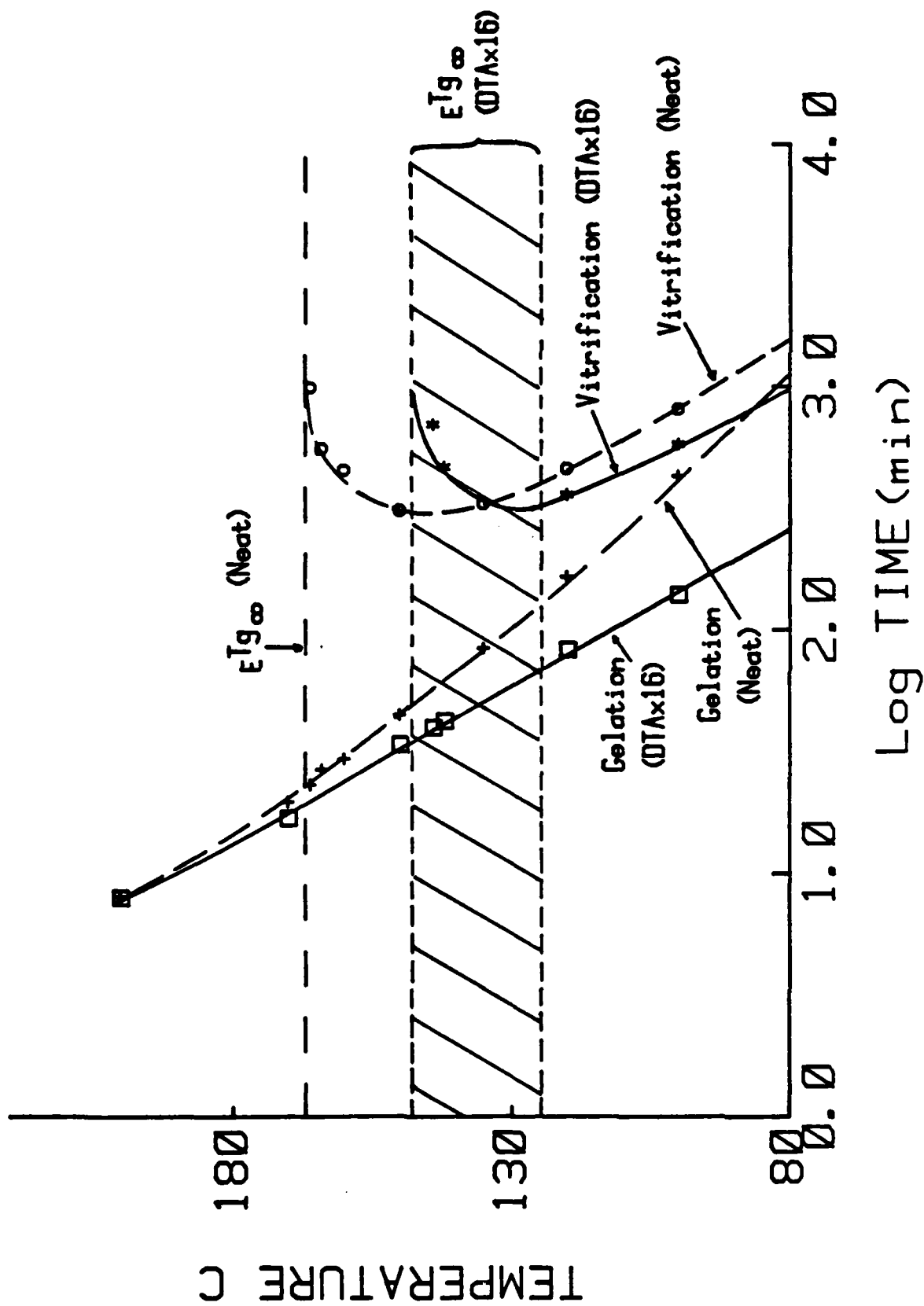
Figure 13

Figure 14

Figure 15

Figure 16

Figure 17

2 μm

(a)

Figure 18

2 μm

(b)
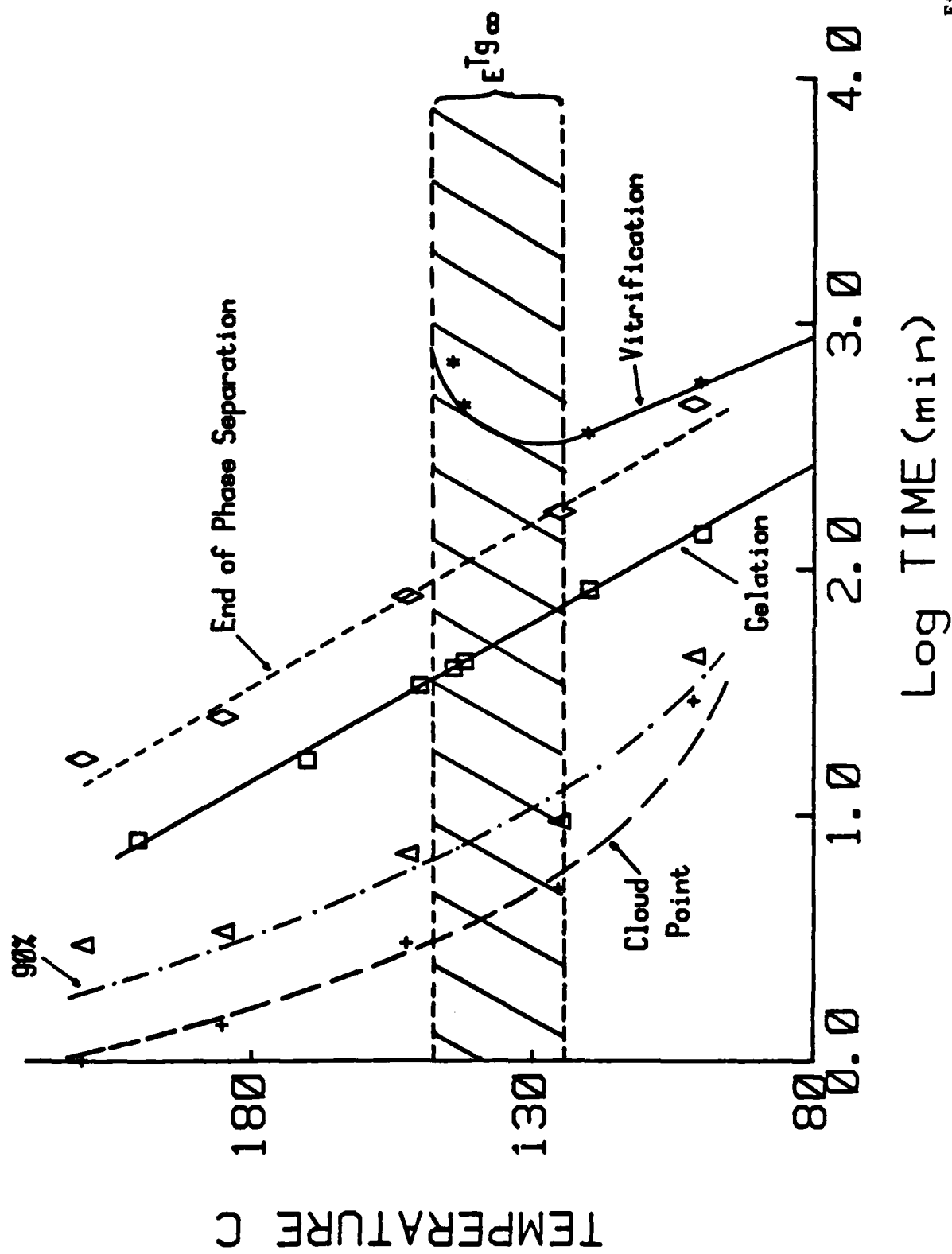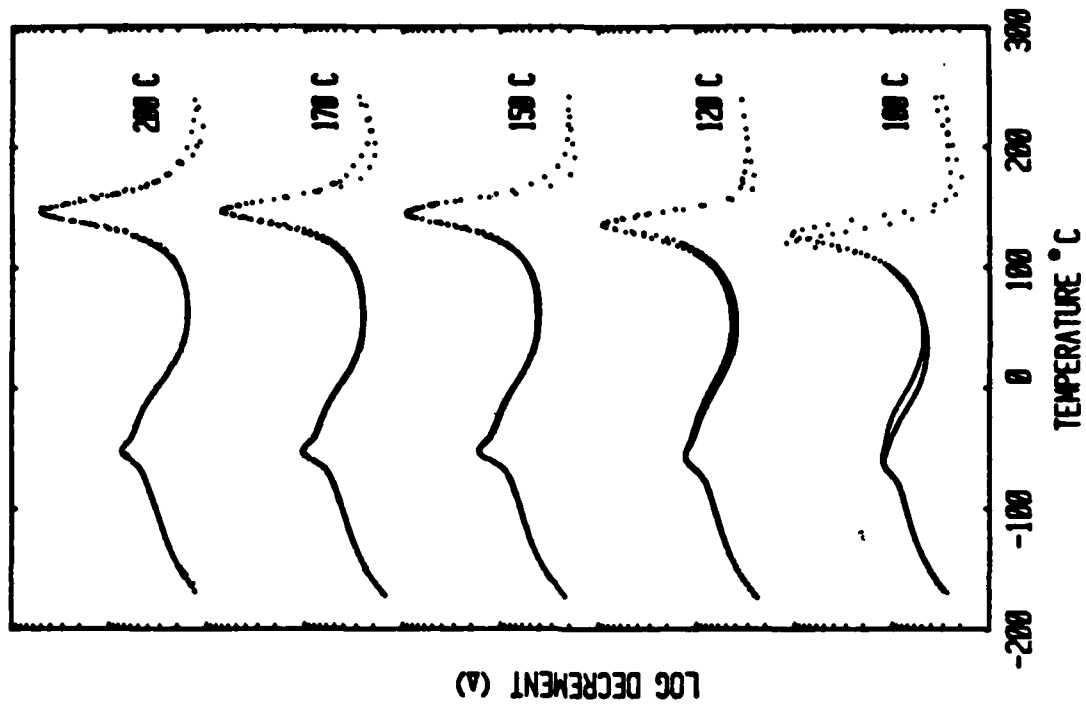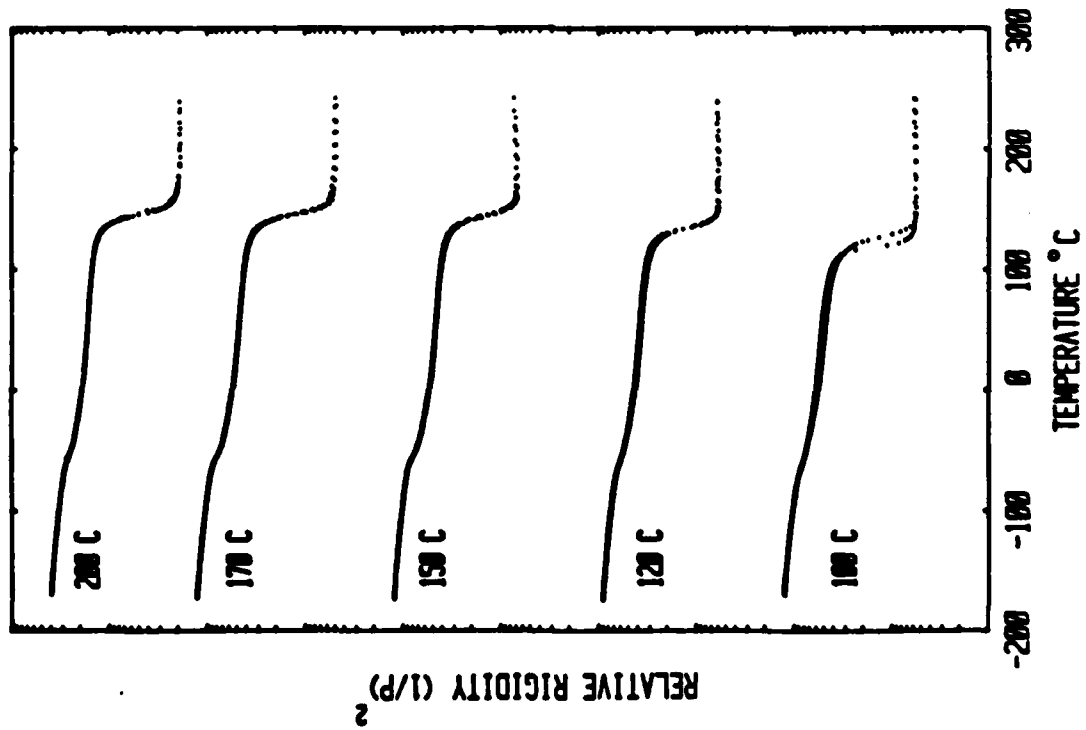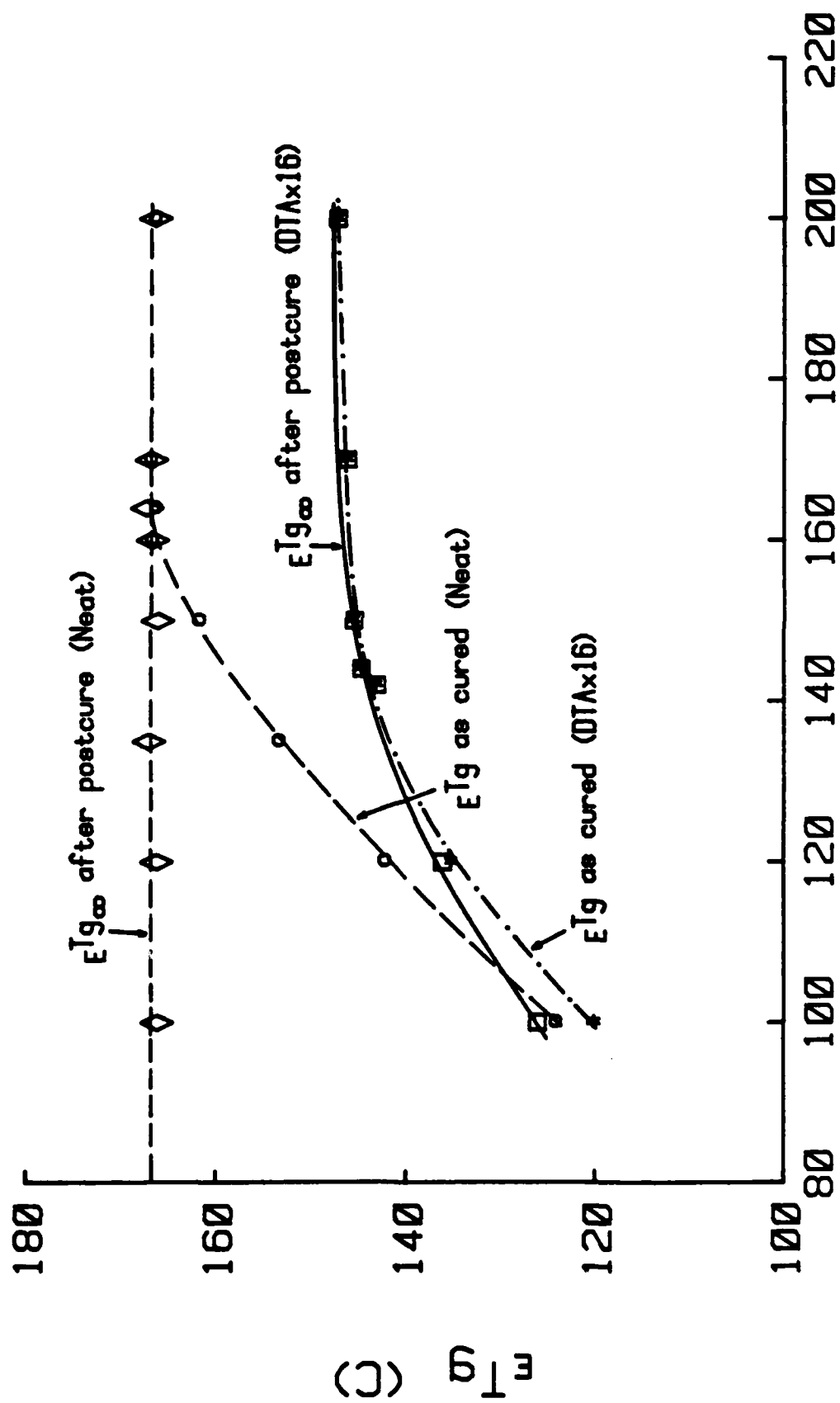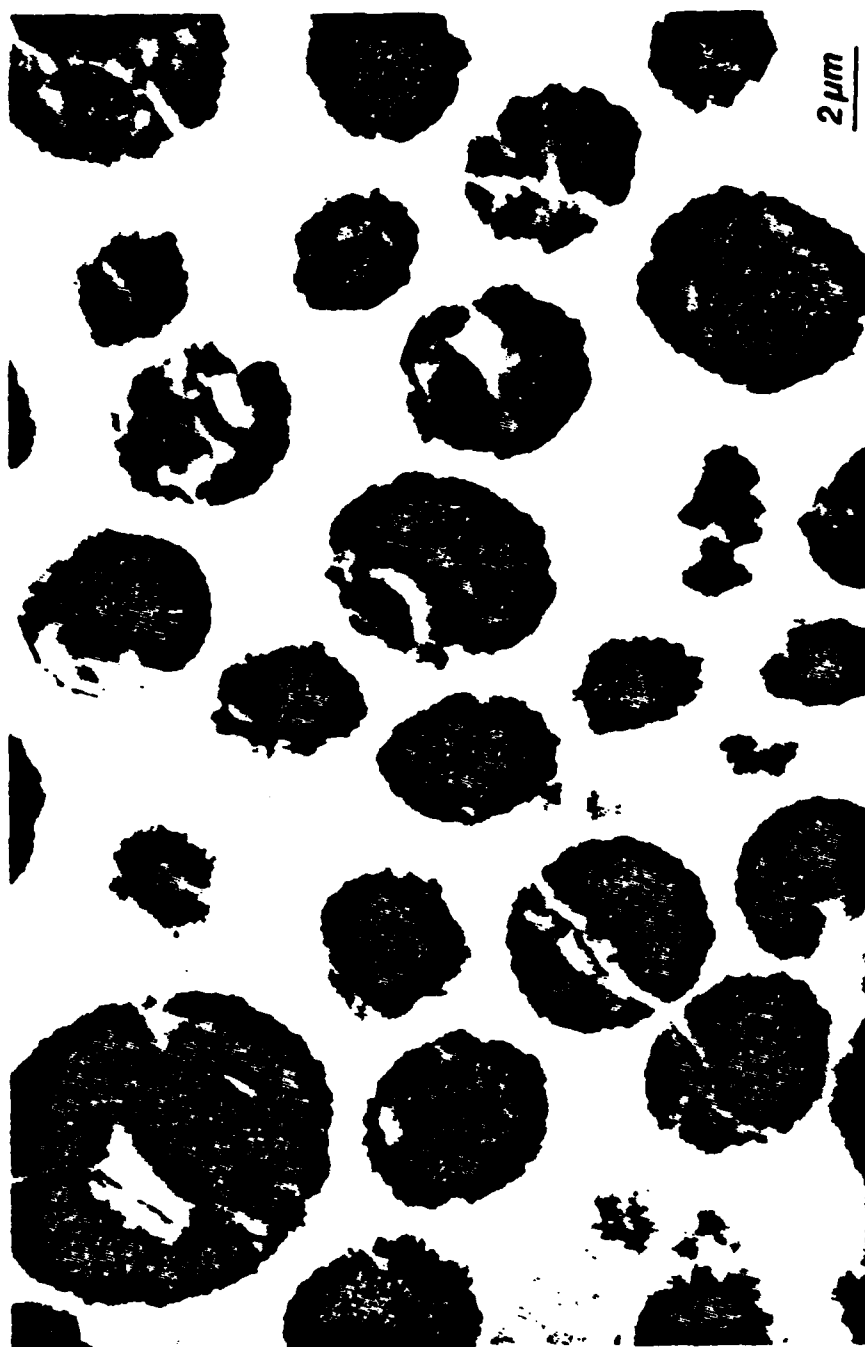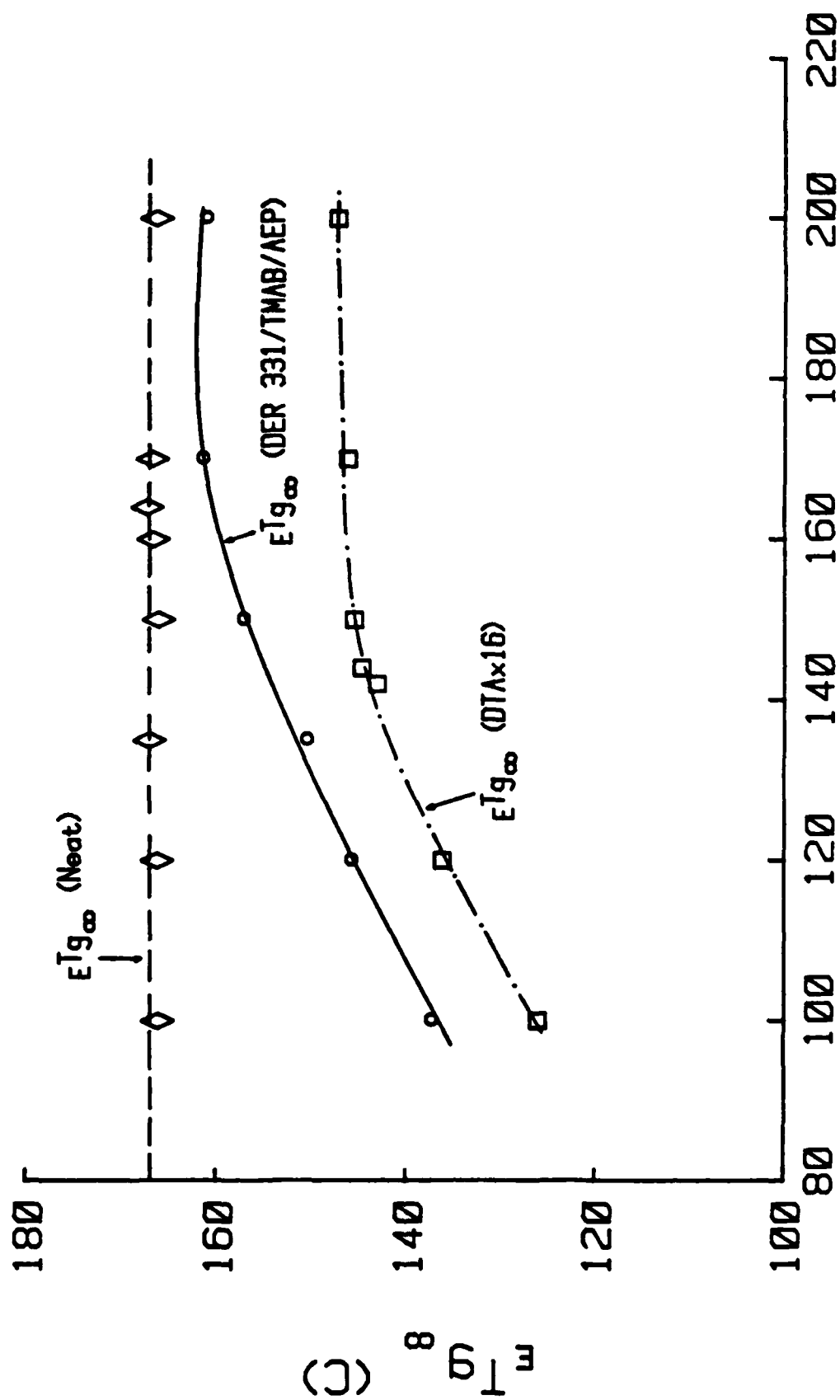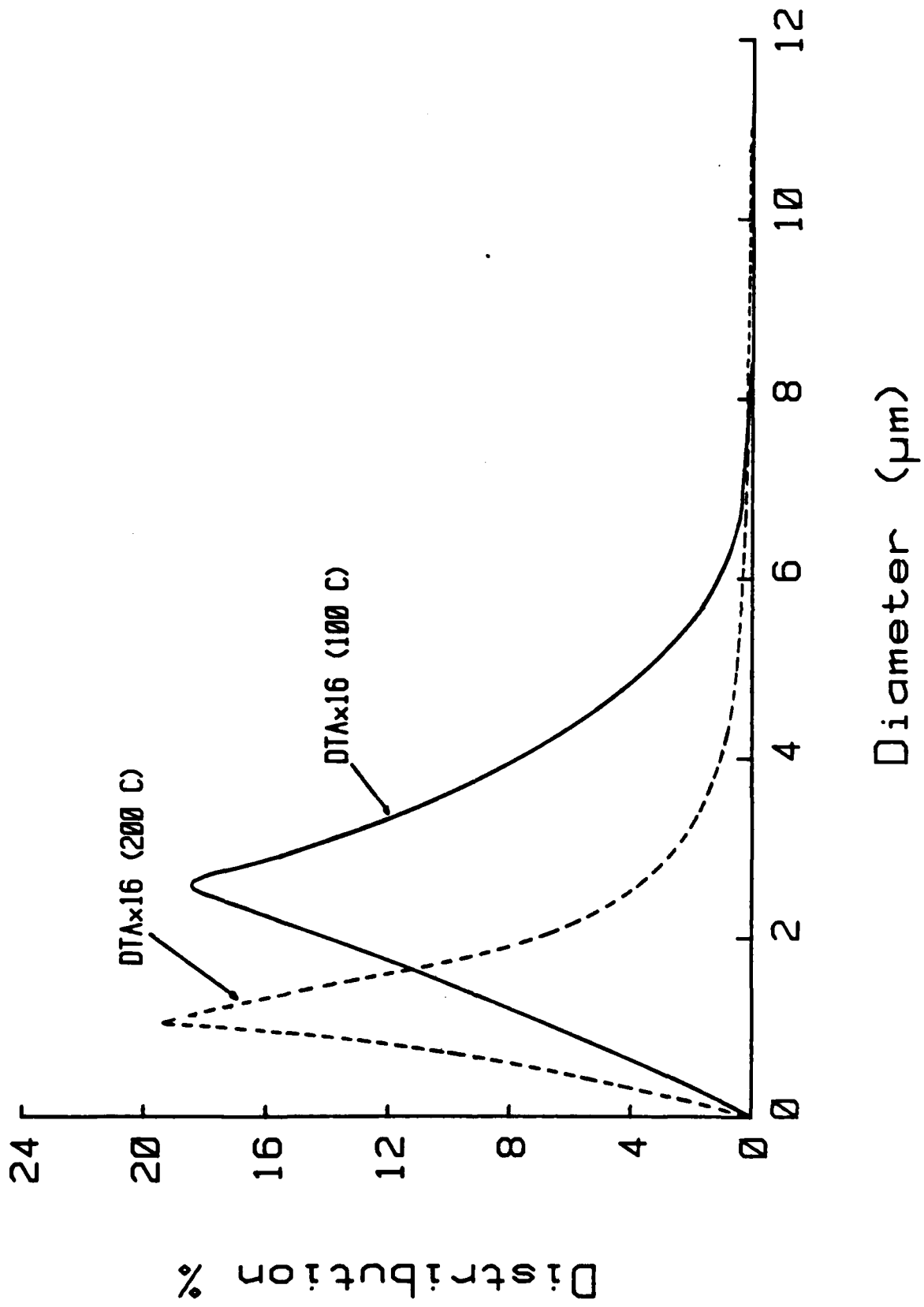
Figure 18

Figure 19

Figure 20

Figure 21

TECHNICAL REPORT DISTRIBUTION LIST, GEN

	No. Copies		No. Copies
Office of Naval Research Attn: Code 413 800 N. Quincy Street Arlington, Virginia 22217	2	Dr. David Young Code 334 NORDA NSTL, Mississippi 39529	1
Dr. Bernard Douda Naval Weapons Support Center Code 5042 Crane, Indiana 47522	1	Naval Weapons Center Attn: Dr. A. B. Amster Chemistry Division China Lake, California 93555	1
Commander, Naval Air Systems Command Attn: Code 310C (H. Rosenwasser) Washington, D.C. 20360	1	Scientific Advisor Commandant of the Marine Corps Code RD-1 Washington, D.C. 20380	1
Naval Civil Engineering Laboratory Attn: Dr. R. W. Drisko Port Hueneme, California 93401	1	U.S. Army Research Office Attn: CRD-AA-IP P.O. Box 12211 Research Triangle Park, NC 27709	1
Defense Technical Information Center Building 5, Cameron Station Alexandria, Virginia 22314	12	Mr. John Boyle Materials Branch Naval Ship Engineering Center Philadelphia, Pennsylvania 19112	1
DTNSRDC Attn: Dr. G. Bosmajian Applied Chemistry Division Annapolis, Maryland 21401	1	Naval Ocean Systems Center Attn: Dr. S. Yamamoto Marine Sciences Division San Diego, California 91232	1
Dr. William Tolles Superintendent Chemistry Division, Code 6100 Naval Research Laboratory Washington, D.C. 20375	1		

END

FILMED

12-84

DTIC